

Post-Glacial Sedimentation in Ossipee Lake, New Hampshire:

Author: James LeNoir

Persistent link: <http://hdl.handle.net/2345/bc-ir:108650>

This work is posted on [eScholarship@BC](#),
Boston College University Libraries.

Boston College Electronic Thesis or Dissertation, 2019

Copyright is held by the author, with all rights reserved, unless otherwise noted.

Post-Glacial Sedimentation in Ossipee Lake, New Hampshire

James LeNoir

A thesis
submitted to the Faculty of
the department of Earth and Environmental Sciences
in partial fulfillment
of the requirements for the degree of
Master of Science

Boston College
Morrissey College of Arts and Sciences
Graduate School

December, 2019

POST-GLACIAL SEDIMENTATION IN OSSIPEE LAKE, NEW HAMPSHIRE

James LeNoir

Advisor: Noah P. Snyder, Ph.D.

Abstract

Land cover and climate changes, attributed to natural and anthropogenic forcings, cause deviations in geomorphic processes that act to deliver sediment from watersheds to lakes. In New England, contradictory evidence exists as to the influence of deforestation associated with EuroAmerican settlement and major flood events on watershed erosion rates over the past ~250 years. Through combining sediment core analysis from Ossipee Lake, New Hampshire with geomorphic analysis of the Ossipee Lake watershed, this study quantifies Holocene through Anthropocene watershed erosion rates, and assesses variations in rates in relation to short-term historic events such as major storm events or deforestation, and long-term variations related to natural climate variability and post-glacial landscape evolution. An 8.63 m core was collected and spans the entire period from deglaciation to present. Bulk composition and age-depth modeling, utilizing both short-lived radioisotopes and radiocarbon dating, are used to quantify changes in deposition and inferred erosion rates over time. Additional insight on sedimentary processes is provided by measurements of magnetic susceptibility and bulk geochemistry. Lake-sediment data suggests clastic sediment mass accumulation rates vary between 0.0032 to 0.5870 g/cm²/yr, with deposits of increased terrestrially derived sediment focused between ~8500 to 7800, ~6500 to 2500, and 1600 cal yr BP to present. Geomorphic analysis is used to identify regions within the watershed that act to deliver sediment to Ossipee Lake. Potential sources of sediment supply include loose, unconsolidated proglacial deposits near Ossipee Lake that transition to primarily till in upland areas. Calculated bed shear stress along rivers highlights areas in the watershed capable of transporting sediment and areas that can serve as traps thus limiting sediment delivery to Ossipee Lake.

ACKNOWLEDGMENTS

I would like to thank Noah Snyder for his guidance, assistance, and insight to this project in addition to my academic experiences as a graduate student. Thank you to Timothy Cook who is one of the people who sparked my research interest in Earth Surface processes and lakes during my undergraduate studies and research, and who has also provided guidance and assistance in this project. Thank you to Jeremy Shakun and Tara Pisani Gareau for serving as committee members. Thank you for my lab group at Boston College and Worcester State University for contributing to field work and research collaboration: Samantha Dow, Xinyi Zeng, Robin Kim, Kay Paradis, and Sarah Jonathon. Thank you to the Department of Earth and Environmental Science at Boston College, who provided me with the opportunity and financial support to pursue this research. Funding for this research was also supported by the Marland Pratt Billings and Katherine Fowler-Billings Research Award and the Department of Interior Northeast Climate Adaption Center.

TABLE OF CONTENTS

Acknowledgments	iv
List of tables.....	vi
List of figures.....	vii
1.0 Introduction	1
1.1 Post-glacial evolution in New England.....	2
1.1.1 Post-glacial vegetation history	5
1.1.2 Post-glacial climate variability and New England sedimentation.....	8
1.2 Project overview.....	11
2.0 Study Area	12
2.1 Human occupation	18
3.0 Methods	23
3.1 Field work	23
3.2 Laboratory analysis	25
3.3 Watershed analysis	31
4.0 Results	33
4.1 Subbottom sonar surveys	33
4.2 Core stratigraphy	33
4.3 South basin core chronology	40
4.4 Ossipee Lake watershed	50
5.0 Discussion.....	52
5.1 Sediment supply from the watershed to Ossipee Lake	52
5.2 Age-depth models.....	53
5.3 Spatial variations in sedimentation within Ossipee Lake.....	56
5.4 Paraglacial sedimentation	58
5.5 Holocene sedimentation	59
5.6 Anthropocene sedimentation.....	62
5.7 Future work.....	66
6.0 Conclusion.....	68
References	72

LIST OF TABLES

Table 1. Ecological communities within the Ossipee Lake watershed	14
Table 2. Summary of all Ossipee Lake sediment cores	24
Table 3. Ossipee Lake composite sediment cores.....	26
Table 4. Event layers recorded in the Ossipee Lake southern composite record.....	37
Table 5. Ossipee Lake radiocarbon samples and results.....	39
Table 6. Ossipee Lake sediment core age-control points.....	42
Table 7. Mean, mininum, and maximum clastic mass accumulation rates.....	48
Table 8. Duration of event layers in the southern composite record	55

LIST OF FIGURES

Figure 1. Study area maps.....	3
Figure 2. Surficial geology of the Ossipee Lake watershed	4
Figure 3. Discharge data from the Bearcamp River, Saco River, Ossipee Lake outlet, and water level data from Ossipee Lake	6
Figure 4. Holocene temperature and effective precipitation.....	7
Figure 5. Aerial photograph of Ossipee Lake	13
Figure 6. Land cover assessment of the Ossipee Lake watershed	16
Figure 7. Longitudinal profiles and shear stress at the bed of major rivers within the Ossipee Lake watershed.....	17
Figure 8. Ossipee Lake water quality data.....	19
Figure 9. Historic topographic map (1861) of Carroll County, NH	21
Figure 10. Farmland area in New Hampshire	22
Figure 11. Ossipee Lake subbottom sonar transects	34
Figure 12. Ossipee Lake southern composite core photograph and geochemical data....	35
Figure 13. Ossipee Lake north and south composite core magnetic susceptibility data...	38
Figure 14. ^{137}Cs and ^{210}Pb activity, ^{210}Pb age-depth model, and bulk Pb counts	41
Figure 15. Age-depth models of the Ossipee Lake southern composite record	44
Figure 16. Linear accumulation rates from the Ossipee Lake south composite record ...	45
Figure 17. Clastic mass accumulation rates from the Ossipee Lake south composite record	47
Figure 18. Event frequency of the Ossipee Lake southern composite record	49
Figure 19. Stone walls within the Ossipee Lake watershed.....	51
Appendix. Section cores that comprise the Ossipee Lake southern composite record....	79

1.0 Introduction

Humans have been argued to be the most important geomorphic agent currently shaping the Earth's surface (Hooke, 1994), as anthropogenic activities modify and commonly degrade the landscape (Hooke, 2012). The extensive impact of humans on the environment and increasing global population accelerates the need to understand how humans alter earth surface processes. Anthropogenic changes can occur directly through landscape modification or indirectly through climate change. In New England, contradictory evidence exists as to the influence of deforestation associated with EuroAmerican settlement and major flood events associated with a wetter climate on watershed erosion rates within the historic record. Through combining sediment core analysis from Ossipee Lake, New Hampshire with geomorphic analysis of its watershed, this study quantifies post-glacial sedimentation in Ossipee Lake to compare pre- and post-settlement inferred watershed erosion rates. The goal of this study is to understand how the Ossipee Lake watershed has responded to changes in climate and land cover following deglaciation, and to what degree human activity has served as a disturbance agent on the landscape. Understanding how the Ossipee Lake watershed responds to changes in climate and land cover provides insight to conservation and remediation practices. Quantification of sedimentation rates provide the opportunity to assess the reforested New England landscape as a means to combat erosion. Comparison between modern sedimentation rates and precipitation can guide potential remediation practices to promote resiliency with respect to erosion under extreme precipitation events.

This study focuses on converting a lacustrine record of sediment mass accumulation to a record of landscape processes to understand how the Ossipee Lake watershed has evolved following deglaciation. Some of the challenges in the using sedimentary records to understand

landscape variability include the short duration of the instrumental record and historic observations, and dealing with uncertainties in estimating ages and interpreting proxies through the prehistoric record. Furthermore, most records provide only a single snapshot of what the landscape may have looked like. Lakes continuously accumulate sediment, and therefore provide excellent records to compare changes in rates and processes through time. Previous studies demonstrate the ability of lakes to capture climate and landscape variability over multiple timescales (Likens & Davis, 1975; Dearing *et al.*, 1987; Bierman *et al.*, 1997; Cook *et al.*, 2015; Marlon *et al.*, 2015; Oswald *et al.*, 2018). In this thesis, I explore some of these constraints and ways to improve interpretations of earth surface processes in their application to understanding the landscape history of the southern White Mountains region of New Hampshire.

1.1 Post-glacial evolution in New England

Retreat of the Laurentide Ice Sheet in New England occurred ~18200 to 12500 calendar years before present (cal yr BP), with retreat within the Ossipee Lake watershed (Fig. 1) likely occurring ~14500 cal yr BP (Ridge *et al.*, 2012). During the late stages of deglaciation, Ossipee Lake was part of a larger ice-dammed glacial lake (Newton, 1974a) formed in a trough-shaped basin resulting from deeply eroded bedrock (Moore & Medalie, 1995), which at some point drained following natural dam failure. Although the extent of Glacial Lake Ossipee has not been thoroughly studied, glacial lake deposits surrounding the modern lake provide evidence for this former larger water body (Fig. 2; Newton, 1974a; Medalie & Moore, 1995; Moore & Medalie, 1995; Sperduto & Nichols, 2004). The center of Glacial Lake Ossipee was estimated to be ~ 85 m deeper than the present lake and rapidly filled with sediment (Medalie & Moore, 1995; Moore & Medalie, 1995). The lake was ponded in front of the melting ice front, shown through the formation of the stratified drift aquifer surrounding the modern Ossipee Lake (Medalie & Moore,

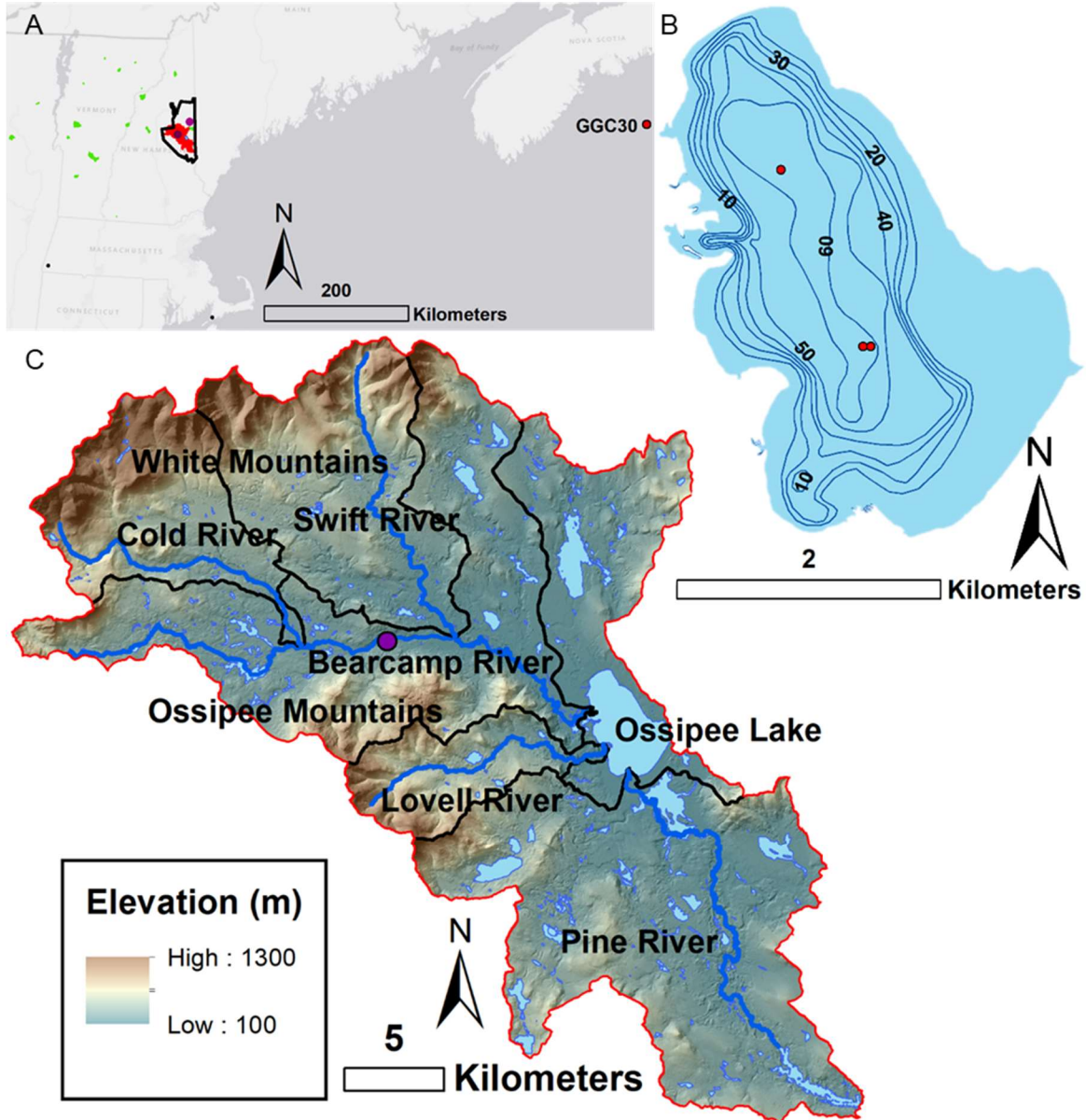


Figure 1. (A) The Ossipee Lake watershed (red; 768 km²), surrounded by the border to Carroll County (black), is a much larger drainage basin compared to sites used to reconstruct Holocene hydrologic events (green; Brown *et al.*, 2000; Noren *et al.*, 2002; Parris *et al.*, 2010) and lake-levels (blue; Newby *et al.*, 2011; Marsicek *et al.*, 2013). Site GGC30 (Sachs, 2007) is represented by a red dot off the coast of Nova Scotia. USGS gage stations used for streamflow analysis are represented by purple dots within Carroll County. (B) Ossipee Lake, contours in feet, is a relatively large lake (13 km²) with a maximum depth of 19.5 m. Coring locations are represented by red dots. Major rivers within the Ossipee Lake watershed (C) include the Pine, Lovell, Bearcamp, Cold, and Swift rivers. The purple dot on the Bearcamp River represents the Bearcamp River gage station.

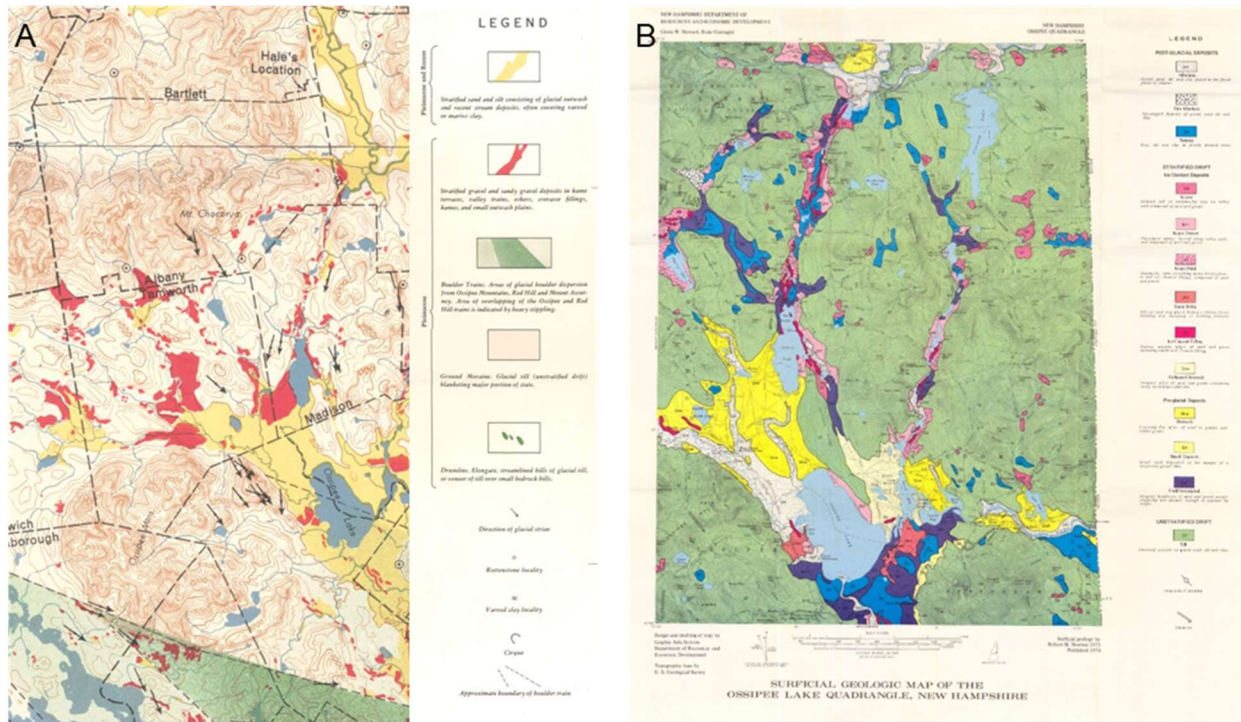


Figure 2. Surficial geologic maps of the Ossipee Lake region include a zoomed-in portion from a state-wide survey (A; Goldthwait *et al.*, 1950) and a more detailed survey of the Ossipee Lake Quadrangle (B; Newton, 1974b). The southern shoreline of Ossipee Lake, and the region surrounding the Pine River, consists of swamp land and irregular landforms of gravel, sand, and silt likely sourced by glacial stream deposits. Northwest of Ossipee Lake and the region surrounding the Bearcamp River and its tributaries consist primarily of post-glacial alluvium (sand, silt, and clay) propagating outwards into proglacial outwash. Till is more common in the upstream reaches of the Ossipee Lake watershed, including the region surrounding the Lovell River and the Ossipee Mountains.

1995; Moore & Medalie, 1995). Kame deltas identified along the western shore and southeast of Ossipee Lake (Fig. 2; Newton, 1974a) further support the presence of a glacial lake in the basin. The elevation of these kame deltas are ~140 to 143 m, and provide an estimated maximum elevation of the glacial lake, whereas the modern lake level fluctuates around 124 m (Fig. 3 A).

1.1.1 Post-glacial vegetation history

During the subsequent thousands of years, the changing New England climate led to pronounced changes in vegetation (Shuman *et al.*, 2005; Oswald *et al.*, 2018). Boreal forest dominated the cool and dry environment from 14000 to 11500 cal yr BP (Oswald *et al.*, 2018). As temperatures began to warm between 12000 to 10000 cal yr BP (Fig. 4), boreal forest was replaced by white pine forest, brought about by further warming and increases in precipitation between 9000 and 8000 cal yr BP (Shuman *et al.*, 2005; Oswald *et al.*, 2018). Hemlock, birch, and beech replaced white pine in inland New England sites during this transition, which persisted through 6000 cal yr BP when temperatures reached the highest values over the Holocene and precipitation remained lower than present. Abrupt cooling between 5500 to 5000 cal yr BP brought about a shift to oak and beech hardwood forests in upland New England sites, which persisted up to 3000 cal yr BP (Oswald *et al.*, 2018). The timing of abrupt cooling also corresponds to decreased water levels in Echo Lake (Shuman *et al.*, 2005). Hemlock recovered in upland sites between 3000 to 2000 cal yr BP, and vegetation shifts towards hemlock and beech over the past millennium are likely the result of late-Holocene trends towards a cooler and wetter climate (Fig. 4). On much more recent timescales, the impact of EuroAmerican settlement is evident in the pollen record, as weedy plants increased during the agricultural era (Donnelly *et al.*, 2015; Oswald *et al.*, 2018).

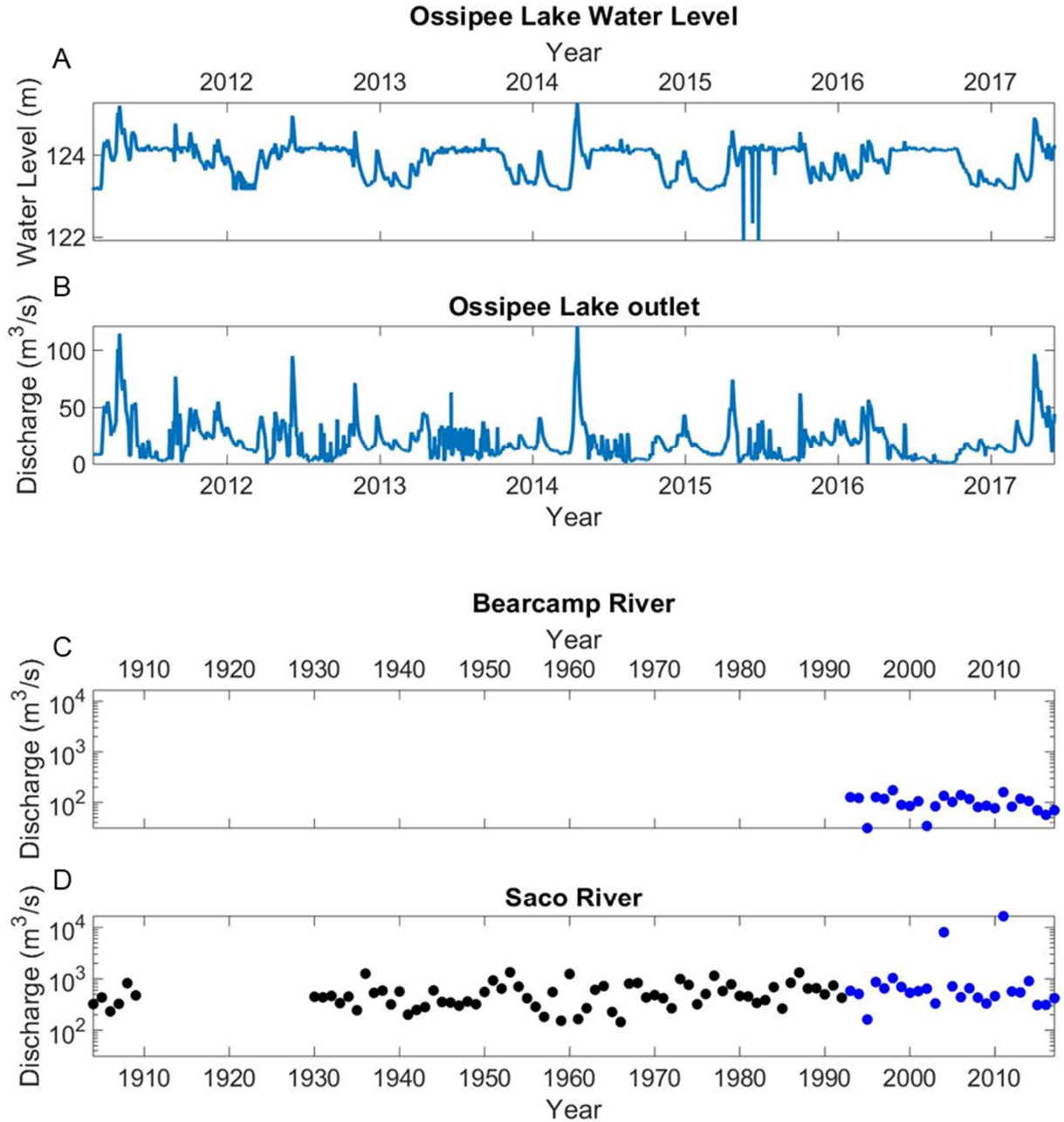


Figure 3. (A) Hourly Ossipee Lake water level recorded from NHDES station along the western shore of Ossipee Lake and (B) streamflow recorded from NHDES gage station along the Bearcamp River ~0.4 km downstream of the Ossipee Lake dam. All available data as of May 31, 2019 are reported here. Peak annual discharge data from USGS gage stations at the Bearcamp River in Tamworth, NH (C; Fig. 1 C) and Saco River in Conway, NH (D; Fig. 1 B). Discharge data for the Saco and Bearcamp rivers were plotted on a log scale because peak streamflow from 2004 and 2011 greatly exceed the other peak discharge data. Dark blue data points correspond to years during which data is available for the Bearcamp River gage station and black data points (D) correspond to data predating recorded data from the Bearcamp River gage station.

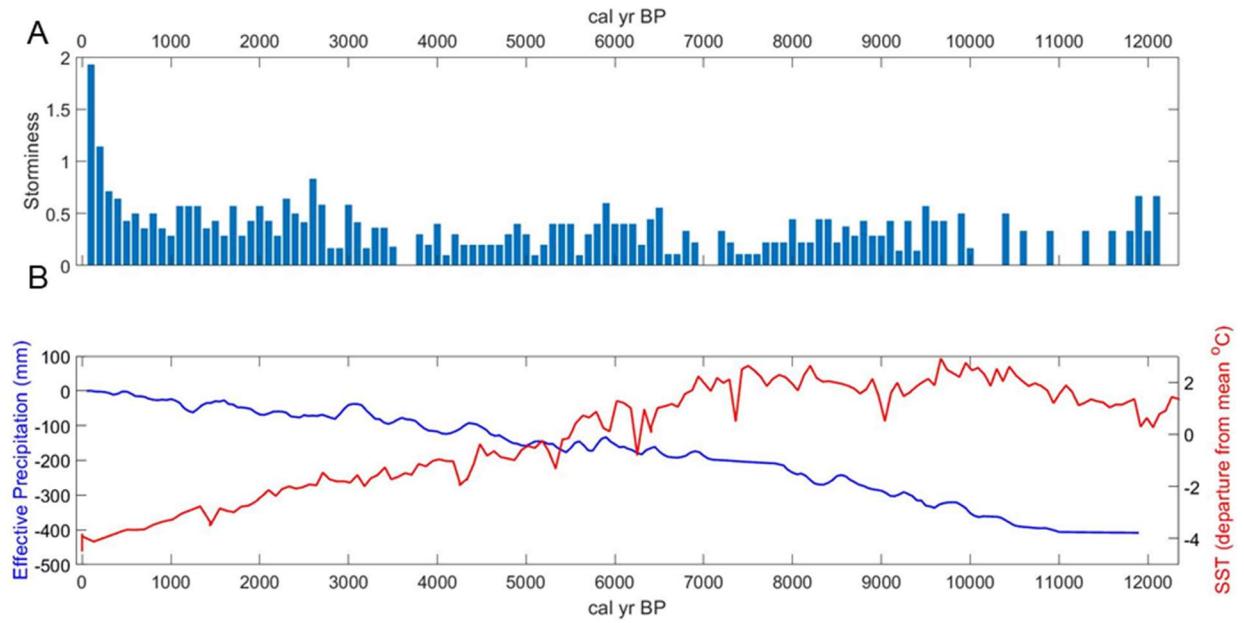


Figure 4. Temperature and precipitation data reconstructed from sediment cores for the northeastern United States (Fig. 1) over the Holocene. (A) Histogram of terrestrially derived sedimentation events (100 year bins) recorded in lakes in New York and Vermont, interpreted as Holocene paleostorms (Noren *et al.*, 2002). (B) Reconstructed effective moisture (blue) from Davis Pond, MA (Newby *et al.*, 2011) and Deep Pond, MA (Marsicek *et al.*, 2013), and sea surface temperature (SST) departure from the mean (red) reconstructed from site GGC30 (Sachs, 2007).

1.1.2 Post-glacial climate variability and New England sedimentation

Temperature in northeastern North America over the past 12000 years peaked during the early to mid Holocene and shows a general decreasing trend (Fig. 4) with millennial-scale temperature variability driven by orbital cycles, and ice sheet loss and subsequent changes in ocean circulation (Viau *et al.*, 2006). Northeastern United States effective moisture generally increased throughout the Holocene (Newby *et al.*, 2011; Marsicek *et al.*, 2013) but contains four periods of prominent low lake-water phases, indicative of multi-century droughts, from 4900 to 4600, 4200 to 3900, 2900 to 2100, and 1300 to 1100 cal yr BP (Newby *et al.*, 2014). Multi-century droughts coincide with cooling in Greenland and provide evidence for circulation changes across the North Atlantic region during this period.

Episodic extreme rainfall over the Holocene has been interpreted from New England lake cores (Brown *et al.*, 2000; Noren *et al.*, 2002; Parris *et al.*, 2010); however, results from existing studies are not entirely consistent. Lake cores from Vermont and upstate New York (Fig. 1 A) suggest periods of increased paleostorms and flooding occurred ~11900, 9100, 5800, and 2100 cal yr BP and are interpreted to be related to variations in the Arctic Oscillation (Noren *et al.*, 2002). Lake cores from New Hampshire and Maine suggest periods of increased paleostorms and flooding occurred ~11500, 8200, 6800, 3900, 3000, 2100, 1400 cal yr BP and are interpreted to have instead been driven by tropical air masses (Parris *et al.*, 2010). Large hydrologic events recorded in Ritterbush Pond, Vermont occurred 9440, 6840, 2620 cal yr BP with the highest frequency of events occurring >8600, 6840 to 6330, and 2620 to 1750 cal yr BP (Brown *et al.*, 2000). Since the late 20th century, increases in the frequency and magnitude of flooding have been linked to variations in the North Atlantic Oscillation (Collins, 2009; Armstrong *et al.*, 2012; 2014).

Long-term trends and abrupt shifts in climate and vegetation impact earth surface processes, as captured in lake sediment records from Mirror Lake, New Hampshire (Likens & Davis, 1975). Deposition rates following deglaciation were the highest recorded in Mirror Lake during the immediate post-glacial period from 11300 to 9300 cal yr BP, interpreted to be linked to the transport of largely unweathered inorganic particulate matter on the unstable landscape within the watershed (Likens & Davis, 1975). Deposition rates then decreased ~9500 to 9000 cal yr BP as vegetation reached its maximum coverage and allochthonous input remained relatively low until the period of EuroAmerican settlement.

Changes in land use, particularly deforestation for agriculture, can have tremendous impacts on earth surface processes (Likens & Davis, 1975; Thorson *et al.*, 1998; Bierman *et al.*, 1997; 2005). Vegetation provides a twofold role for limiting erosion. Roots serve to stabilize soil, requiring stronger shear forces to drive sediment mobility, and increase water infiltration and storage capacities thus reducing runoff. Runoff generated by storms can result in increased erosion within watersheds. Three processes of storm runoff dominate in humid, forested areas: subsurface storm flow, return flow, and direct precipitation on saturated land (a specific type of overland flow) (Dunne *et al.*, 1975). Under saturated conditions, the infiltration capability of soil decreases and hydraulic conductivity increases, resulting in higher runoff ratios (Favaro & Lamoureux, 2014).

EuroAmerican settlement in New England resulted in peak deforestation during the late 19th century that culminated in 80 percent loss in forest cover (Foster, 1992). The removal of forest through clear cutting and agricultural practices during EuroAmerican settlement decreased hillslope stability and triggered aggradation on valley-bottom alluvial fans in northern Vermont (Bierman *et al.*, 1997). Analysis of historic photographs from 1860 to 1990 in Vermont further

demonstrate erosion is more common in clear-cut areas compared to partially or fully forested sites (Bierman *et al.*, 2005). Analysis of sedimentary records and hydrologic modelling from Lebanon, Connecticut (Thorson *et al.*, 1998) indicate the modern sediment budget, flood regime, and riparian habitat of wetlands continue to be driven from the initial pulse of colonization from 1695 to 1787. More recent studies conversely suggest sedimentation events in certain New England watersheds are more sensitive to antecedent soil moisture conditions and large-scale flood events rather than land-use change (Brown *et al.*, 2000, 2002; Cook *et al.*, 2015; Yellen *et al.*, 2016).

Increasing precipitation trends since the turn of the 20th century have been linked to increases in erosion. Sediment core analysis from Amherst Lake, Vermont, (Cook *et al.*, 2015) and the tidal zone of the Connecticut River and an upland tributary (Yellen *et al.*, 2016) suggest 20th century catastrophic erosion events are driven by intense flooding modulated by antecedent moisture. The magnitude of these erosion events, especially the erosion associated with Tropical Storm Irene in 2011, drastically exceed those associated with EuroAmerican land use during the 19th century.

Increased frequency and magnitude of precipitation associated with natural variations poses larger implications when considering the potential anthropogenic influences associated with climate change. Climate projections demonstrate increased global temperatures, mean precipitation, and frequency and magnitude of extreme precipitation focused in high-latitude regions, the equatorial Pacific, and mid-latitude wet regions (IPCC, 2014), suggesting Irene-like erosion events may become more frequent (Cook *et al.*, 2015). Modeling efforts in western Europe (Ward *et al.*, 2009) demonstrate the influence of climate and land use on suspended sediment yield. Land use was found to be the primary control on long-term variations in

suspended sediment yield, with a wetter climate causing deforested land to be more sensitive to erosion. The modeled results highlight the applicability of land-use practices in certain catchments as a mechanism to reduce suspended sediment yield, and subsequently erosion, with projections toward a wetter climate.

1.2 Project overview

The discrepancy in how human activity has influenced the sedimentary record in New England motivated this study. Holocene through Anthropocene inferred watershed erosion rates were quantified from Ossipee Lake sediment cores to answer two research questions:

1. Is sediment accumulation in Ossipee Lake over the past 250 years anomalous compared with the rest of the Holocene?
2. Is the primary driver of watershed erosion rates over the past 250 years deforestation and anthropogenic changes to the landscape, or intense flood events modulated by antecedent moisture conditions and large-scale storms associated with increasing precipitation trends?

As this project developed, additional research questions were explored:

3. What implications do different age-depth modelling techniques have on estimated sedimentation rates and inferred watershed erosion rates?
4. How have inferred watershed erosion rates varied through the entire post-glacial period?

Research question 3 arose due to varying results observed when applying different statistical approaches to construct age-depth models of Ossipee Lake sediment cores. Age-depth modelling is a commonly applied technique in paleolimnological studies, and is required to

provide a means of interpolating ages, and associated uncertainty, for intervals between dated horizons, from which accumulation rates are subsequently derived. Age-depth modelling techniques are often simplified or not well documented in the literature (Blaauw, 2010), and while more rigorous models have been proposed (Ramsey, 2008; Blaauw & Christen, 2011), they are often more complicated and still have inherent problems reconstructing ages. Even though age-depth modelling has made advancements in recent years to produce more environmentally realistic models, they can still result in the underestimation or overestimation of sediment accumulation rates (Trachsel & Telford, 2017). Research question 4 was explored because of the successful collection of a continuous sediment core record that captures the entire post-glacial sequence.

2.0 Study Area

The Ossipee Lake watershed is an ideal landscape to quantify changes in post-glacial sedimentation and compare pre- and post-settlement inferred watershed erosion rates. The watershed is dominantly underlain by unconsolidated sediment that can be reworked during a disturbance (Fig. 2). The presence of deltas at the mouths of inlet rivers (Fig. 5) suggest sediment mobilized from the watershed is being delivered to Ossipee Lake. Additionally, known EuroAmerican settlement within the watershed provides the basis for potential human disturbances during this period.

The Ossipee Lake watershed (Fig. 1; 768.4 km²) is in eastern New Hampshire and encompasses the towns of Ossipee, Albany, Effingham, Freedom, Madison, Moultonborough, Sandwich, Tamworth, Wakefield, Waterville Valley, Wolfeboro, and Brookfield. The primarily forested watershed consists of numerous ecological communities (Table 1; Sperduto & Nichols,

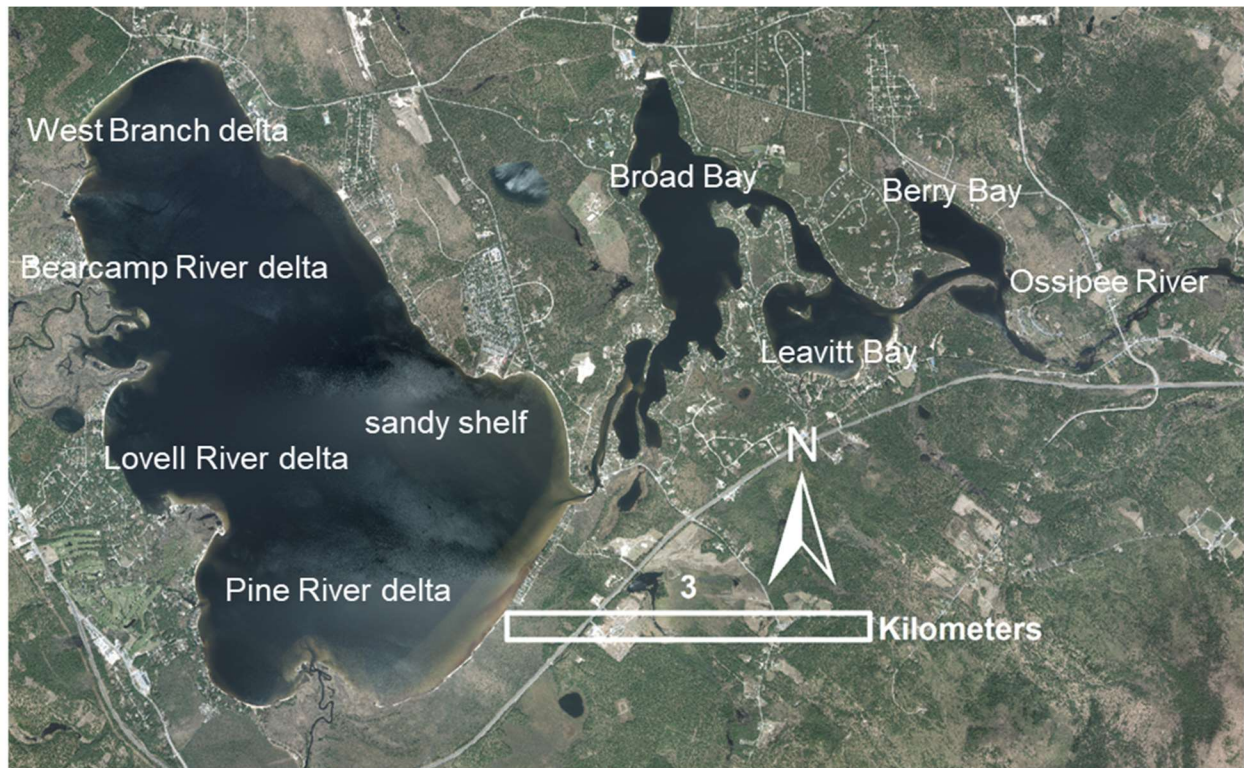


Figure 5. Aerial photograph (2011) of Ossipee Lake captures the deltas formed at the mouths of the inlet rivers and the sandy shelf at the outlet of Ossipee Lake, which feeds the Broad, Leavitt, and Berry outlet bays and the Ossipee River.

Table 1. Examples of ecological communities found within the Ossipee Lake watershed (Sperduto & Nichols, 2004). A large variety of natural communities are found on lowland proglacial sediments.

Natural Community	Soil description	Example Location
Hemlock-white pine forest	Dry-mesic and infertile till.	Pine River Esker (Ossipee) and Hemenway State reservation (Tamworth)
Mixed pine-red oak woodland	Coarse, light textured glacial sand plain at low elevations	Throughout southern part of Ossipee Lake watershed
Balsam fir floodplain/silt plain	Silt plains derived from glacial lakebed deposits and stream deposits	Pine River (southern Ossipee Lake watershed)
Herbaceous seepage marsh	Marshland consisting of shallow peat over silt or silty muck shallow peat or	Southern area of Ossipee Lake
Sweet gale-alder shrub thicket	Forms alongside and top of sandy ice berms on large lakes	Southern shore of Ossipee Lake
Liverwort-horned bladderwort fern	Kettle holes and peatland basins	Pine River State Forest (southern part of watershed)

2004). Hardwood forests compose the majority of the watershed, and the northern portion of the Ossipee Lake shoreline is composed of pitch pine and the southern portion of the shoreline consists of forested wetlands (Fig. 6).

The southern portion of the White Mountains (up to 1269 m) define the northern border of the Ossipee Lake watershed. The Ossipee Mountains (up to 611 m) are in the westernmost portion of the watershed and are a circular shaped ring-dyke with an average diameter of 14.5 km (Wilson, 1937; Sperduto & Nichols, 2004). The bedrock geology belongs to three groups: (1) Early Devonian Littleton Formation, (2) mid-Devonian New Hampshire Plutonic Series, and (3) Early Jurassic White Mountain Plutonic-Volcanic Series (Wilson, 1937).

Thick surficial deposits surround Ossipee Lake, providing an abundant source of sediment. These mostly sand and gravel sized sediments compose ice contact deposits, proglacial outwash, and post-glacial alluvium which transition to predominately till in upland areas (Fig. 2). Orientations of drumlins and ice-contact faces within the watershed indicate general north to northwesterly retreat of ice (Newton, 1974a).

The West Branch, Bearcamp, Lovell, and Pine rivers act to transport sediment to Ossipee Lake as evident by deltas formed at the mouths of these rivers along the western and southern shorelines of Ossipee Lake (Figs. 1 and 5). The Bearcamp River enters along the western shore and has several major tributaries including the Cold and Swift rivers that originate in the White Mountains. Near the inlet, the Bearcamp River is shallow and slow flowing with a sandy bottom; however, gravel bedded and bedrock reaches with faster streamflow exist farther upstream. The Lovell River is shorter and steeper compared to the Bearcamp River (Fig. 7), enters the lake just south of the Bearcamp River, and originates in the Ossipee Mountains. The Pine River is the

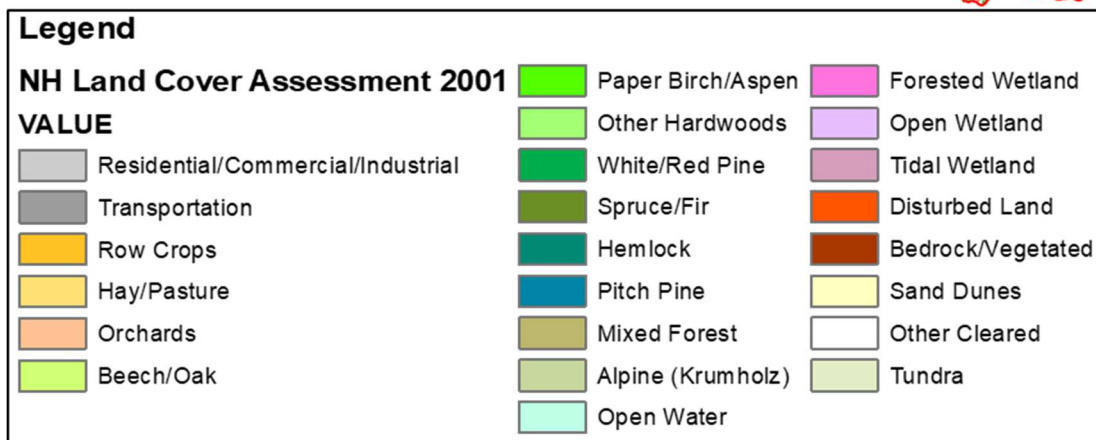
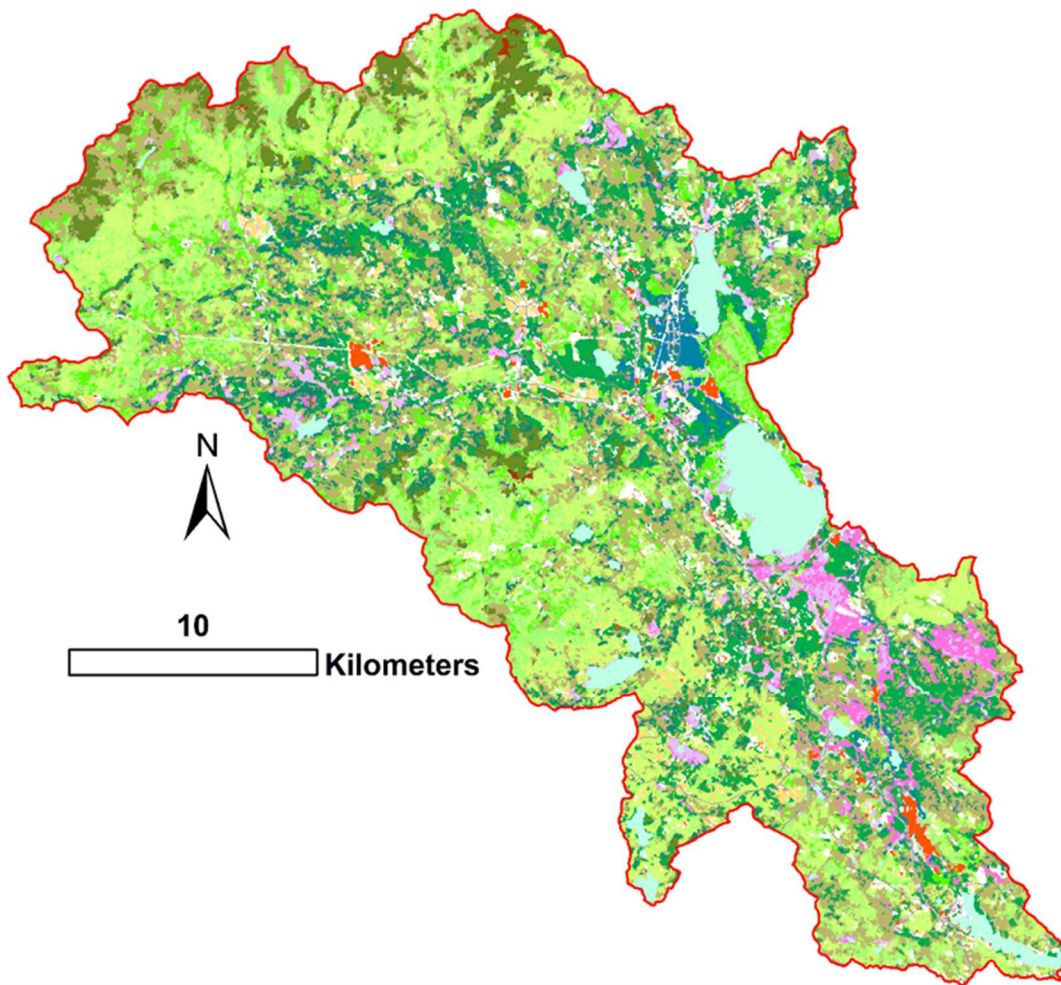


Figure 6. New Hampshire land cover assessment from 2001, made available by NH Granit (University of New Hampshire, 2002) highlights the present predominance of forests and wetlands within the Ossipee Lake watershed, with minimal disturbed land.

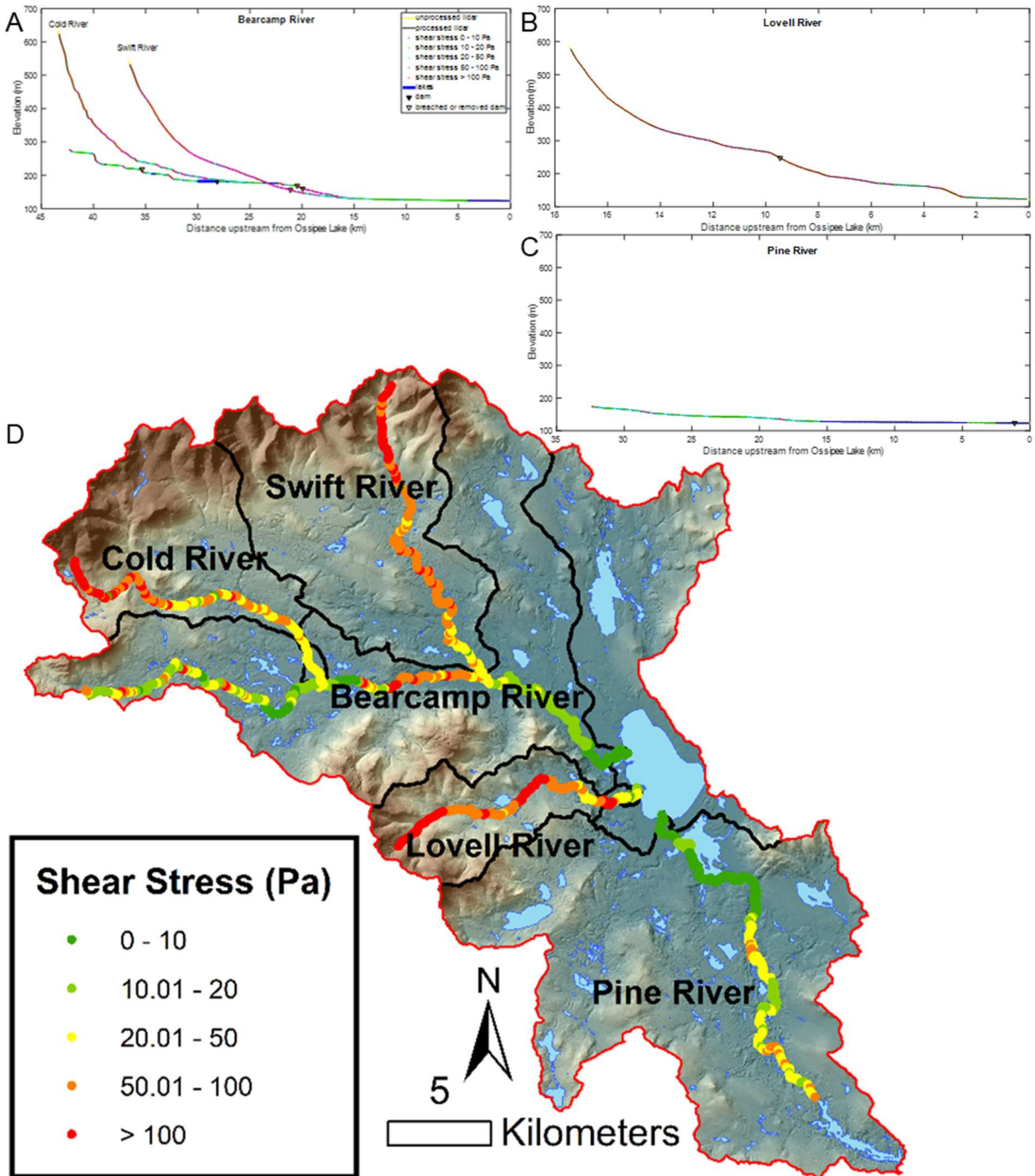


Figure 7. Longitudinal profiles of the Bearcamp River including the Cold and Swift river tributaries (A), Lovell River (B), and Pine River (C). The yellow lines represent the raw, unprocessed longitudinal profile while the black lines represent a processed longitudinal profile that removes minor changes in elevation related to anthropogenic structures such as roads or dams. Shear stress values are plotted from low values (blue) to high values (red). Map of plotted shear stress values (D) ranging from low shear (green) to high shear (red). Areas of high τ_b are found in on steep terrain and represent areas more capable of transporting sediment.

southernmost inlet and is a low-gradient, slow flowing river with vegetated banks. The smaller West Branch (~8.5 km length) enters Ossipee Lake along the northern shoreline.

The maximum depth recorded during bathymetric surveys of Ossipee Lake (13 km²) is 19.5 m, and the mean depth reported by New Hampshire Department of Environmental Services is 8.5 m (2017). During the summer, Ossipee Lake is thermally stratified, and in June 2017 the surface mixed layer was 23 °C and extended to ~ 3 m depth (Fig. 8 A). The thermocline extended from 2.9 to 4.8 m depth with a minimum temperature of 8.8 °C. Dissolved oxygen decreases down the water column with 68.2 % dissolved oxygen saturation at 19 m (Fig. 8 B). The mean conductivity was 38.4 microsiemens per cm indicating very dilute water (Fig. 8 C). The recorded secchi depth was 4.3 m and pH was measured to be 6.9.

The Ossipee River is the outlet of Ossipee Lake, on the southeast shoreline, and is a tributary of the Saco River in western Maine. A large sandy shelf (~2.4 km²; Newell, 1960) is present near the outlet (Fig. 5). The shelf likely formed succeeding the last glaciation, as sand deposited during deglaciation was transported into Ossipee Lake then along the shorelines via littoral drift and longshore currents driven by southwesterly, westerly, and northwesterly winds (Newton, 1974a).

2.1 Human occupation

The Ossipee Native American tribe, a branch of the Abnaquis, inhabited the Ossipee Lake watershed prior to EuroAmerican settlement (Merrill, 1889). Native American food sources included fishing, hunting, nuts, berries, roots, corn, acorns, squashes, and beans (Merrill, 1889). However, beginning in the mid-17th century, early EuroAmerican settlement brought devastating war to the Native American tribes, forcing the Ossipee tribe out of their homeland. As Native

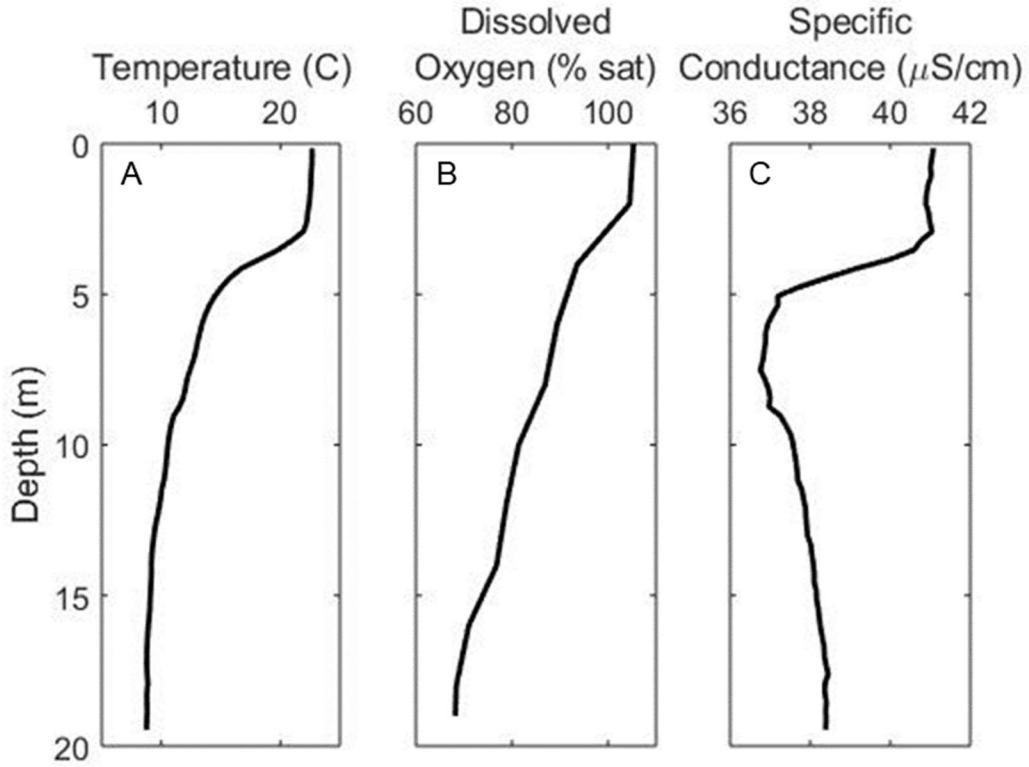


Figure 8. Water quality data, collected on June 22, 2017, include temperature (A), dissolved oxygen (B), and specific conductance (C) collected using conductivity, temperature, and depth instrumentation. Dissolved oxygen was collected using a dissolved-oxygen instrument.

American populations within the Ossipee Lake watershed rapidly decreased, EuroAmerican settlement rapidly increased. By the late-18th century, the towns of Sandwich, Moultonborough, Tamworth, and Wolfeborough were granted (Merrill, 1889). Early EuroAmerican inhabitants were small farmers with typical crops including grain and corn, with pasture land used to support the need for wool. Settlement brought about rapid increases in population and industrialization, with subsequent deforestation.

By 1790, the population in Carroll County (Fig. 1 A) had grown 200 percent in 15 years to 4,850 people. Large-scale settlement occurred by the 19th century when population peaked at 20,465 people in 1860, constructing numerous mills along rivers and clearing much forest for pastures (Merrill, 1889). A historic topographic map of the Ossipee Lake area from 1861 displays the extent of rural industrialization, showing numerous residencies and paper and saw mills within the watershed (Fig. 9).

Populations in Carroll County decreased following 1860, dropping to 18,291 people in 1880 (Merrill, 1889). During the mid to late 19th century, greater than half of the New Hampshire landscape was dedicated to farmland, followed by a relatively rapid decrease in farmland coverage during the early 20th century (Fig. 10). In 1880, Carroll County had 2,758 farms, with 50 % of the surveyed county being improved land, 3 % unimproved land, and 47 % remained mountain, woodland, and forest (Merrill, 1889). Sheep population in New England decreased during the mid-19th century (Perello, 2015). Following farmland abandonment, hardwood forests returned as the dominant land cover. Disturbed land, defined as areas where vegetation or Earth's surface has been altered such as for gravel pits or quarries, accounts for 0.4 % of the watershed (University of New Hampshire, 2002). Within Carroll County, residential land accounts for 0.8 %, transport accounts for 1.8 %, crops account for 0 %, pasture accounts for 1.6 %, and orchards

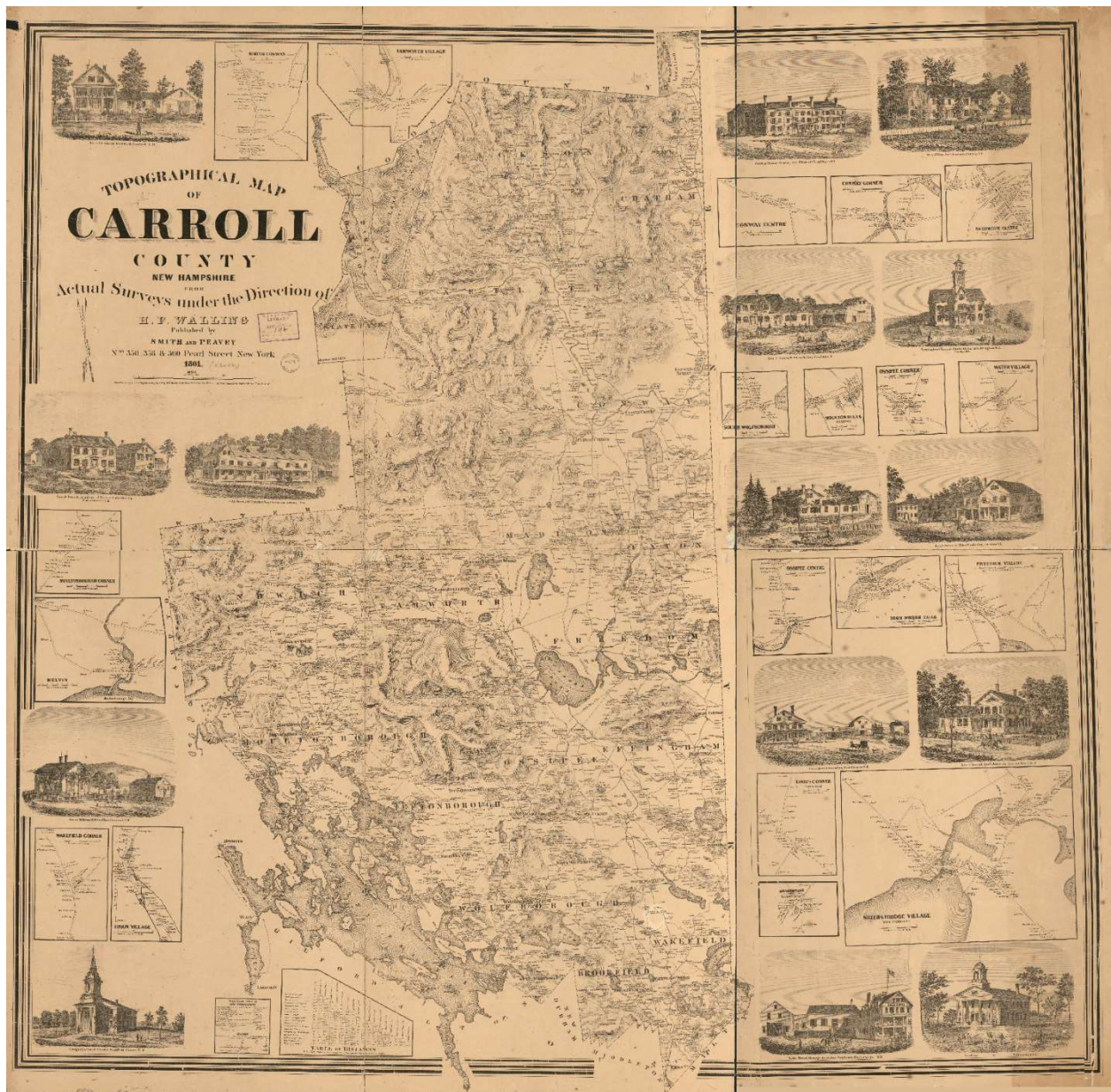


Figure 9. Historic topographic map (Woodford & Smith & Peavey, 1861) of Carroll County from 1861 captures the locations of numerous paper and saw mills, roads used for logging, residencies, and town centers.

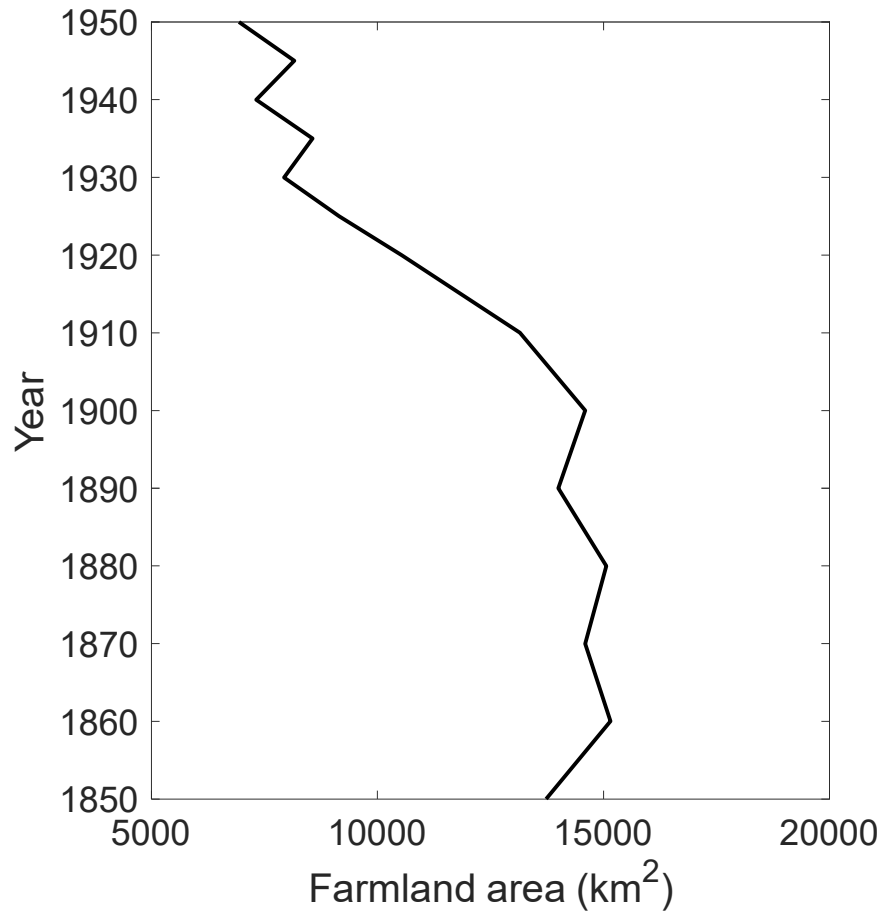


Figure 10. Farmland area in New Hampshire, obtained from the United States Department of Agriculture, Census of Agriculture Historical Archive: (<http://agcensus.mannlib.cornell.edu/AgCensus/homepage.do>).

accounts for 0 % of land coverage (University of New Hampshire, 2002). Recreational use on Ossipee Lake is relatively high during the summer months and houses surround the lake except along the conserved southern shoreline.

Ossipee Lake was previously cored in a study that analyzed how climate and land-use history affect water quality in Squam and Ossipee lakes (Perello, 2015). Four cores were collected from Ossipee Lake extending a maximum length of 57 cm, which was interpreted to represent the year 1660. Perello (2015) used measurements of particle size, organic composition, geochemistry, and diatom communities as proxies for water quality. Diatom assemblages indicate warmer temperatures since the 20th century and grain size was found to increase from 1800 to 1900, and during extreme precipitation events. Changes in sedimentological properties show greater land disturbance early in the record, during a period of high agricultural production and human population, producing a landscape more susceptible to extreme precipitation. This pattern was more prominent in the Squam record compared to Ossipee, and was attributed to the smaller ratio of watershed area to lake area at Squam Lake (Perello, 2015).

3.0 Methods

3.1 Field work

Field work in Ossipee Lake was conducted during the summers of 2017 and 2018. Subbottom sonar surveys were conducted using a SyQuest StrataBox HD single frequency subbottom sonar using a frequency of 10 kHz. Bathymetric data was collected using Lowrance combination GPS/water depth logging sonar.

Surface lake sediment cores (17-1, 17-2, 17-3, 18-3; Table 2; Appendix) range from 0.55 to 2.155 m length and were collected using a gravity-percussion corer. Sediment cores 17-3 (0.55

Table 2. Summary of all Ossipee Lake sediment cores.

Core ID	Basin	Latitude	Longitude	Date collected	Core length (cm)
17-1	South	43.78607199	-71.13875826	June 22, 2017	68
17-2-1	South	43.785935	-71.13881	June 22, 2017	96
17-2-2	South	43.785935	-71.13881	June 22, 2017	119.5
18-1-1-1	South	43.786	-71.138	June 5, 2018	115
18-1-1-2	South	43.786	-71.138	June 5, 2018	116
18-1-2-1	South	43.786	-71.138	June 5, 2018	127.5
18-1-2-2	South	43.786	-71.138	June 5, 2018	162.5
18-1-3-1	South	43.786	-71.138	June 5, 2018	151
18-1-3-2	South	43.786	-71.138	June 5, 2018	138
18-2-1-1	South	43.786	-71.138	June 5, 2018	138
18-2-1-2	South	43.786	-71.138	June 5, 2018	138
18-2-2-1	South	43.786	-71.138	June 5, 2018	138
18-2-2-2	South	43.786	-71.138	June 5, 2018	138
17-3	North	43.80248	-71.14989	June 22, 2017	55
18-3-1	North	43.802	-71.150	June 7, 2018	102
18-3-2	North	43.802	-71.150	June 7, 2018	94.5

m) and 18-3 (1.965 m), were collected from the northern coring location during the summers of 2017 and 2018, respectively (Fig. 1 B). Sediment cores 17-1 (0.68 m) and 17-2 (2.155 m) were collected during the summer of 2017 from the southern coring location. Intact sediment-water interfaces were confirmed in these surface cores by the presence of clear water overlaying sediment surfaces visible through clear coring tubes. A Uwitec multi-drive percussion corer was used to collect two cores (18-1 and 18-2) with multiple overlapping sections spanning different depths below the lake bed ranging from 0.10 to 8.63 m from the southern coring location.

3.2 Laboratory analysis

Cores were split using nondestructive methods to minimize sediment disturbance and loss. Cores were then photographed and visually described using laboratory facilities at UMass Amherst and Worcester State University. Magnetic susceptibility was measured using a Bartington MS2E sensor (Dearing, 1999) at 0.5 cm intervals using split-core logging methodology (Nowaczyk, 2001). An ITRAX core scanner was used to measure bulk element abundances through X-ray fluorescence (XRF) using a Mo tube at 0.1 cm intervals with 30 kV voltage and 55 mA current. Exposure times for cores 17-2, 18-1, 18-2, and 18-3 were 10 s and 15 s for cores 17-1 and 17-3. X-radiographs were obtained from the ITRAX core scanner. Loss on ignition (LOI) is a measure of the percent organic matter within a sample. Dry sediment bulk density and LOI were quantified following standard procedures (Dean, 1974), using 1 cm³ samples collected every cm.

Cores collected from the north and south basins were spliced into composite records for each location by aligning distinguishing visual characteristics and geochemical sediment data between overlapping sections. The northern composite record spans 2.315 m and the southern composite record spans 8.63 m (Table 3). The northern composite record was photographed and

Table 3. Sediment cores spliced into the north and south basin composite core records.

Core ID	Basin	Section start depth (cm)	Section end depth (cm)	Composite start depth (cm)	Composite end depth (cm)
17-2-1	South	0	96	1	96
17-2-2	South	0	110	96.5	206
18-2-1-2	South	6.5	107.5	206.5	307.5
18-1-2-1	South	20	105.5	308	393.5
18-2-2-1	South	21	139	394	512
18-2-2-2	South	0	91.5	512.5	604
18-1-3-1	South	30.5	151	604.5	725
18-1-3-2	South	0	138	725	863
17-3	North	0	42	0	42
18-3-1	North	7.5	102	42.5	137
18-3-2	North	0	94.5	137.5	231.5

measurements of magnetic susceptibility were obtained to compare characteristics with the southern composite record. These two cores were compared to ensure signals recorded within lake cores are attributed to basin wide sedimentation events rather than localized events associated with river deltas and inner lake dynamics such as slumps. The southern composite record was subjected to all methods discussed in this section and was deemed the best site to document terrestrial sediment deposition while minimizing inner-lake dynamics by maximizing the distance between deltas and coring location.

Erosion event layers in previous New England studies have been identified as anomalously dense, enriched in clastic material (low LOI and high magnetic susceptibility), and enriched in potassium (K). Increases in K have been attributed to unweathered, clay-sized particles derived from the mass wasting of glacial legacy sediments stored in upland catchments (Yellen *et al.*, 2014; Cook *et al.*, 2015). Non-event sedimentation is described by dark brown, homogenous gyttja that is enriched in organics. Events deposits were identified in Ossipee cores as layers based on the following criteria: at least 2 cm thick of denser, clastic sediment represented by (1) visual transitions to light brown sediment; (2) denser X-radiograph images; (3) bulk sediment density, magnetic susceptibility, and K counts above a moving 25 cm mean; (4) and LOI below a moving 25 cm mean.

Age-control points were obtained through gamma spectrometry and radiocarbon analysis. Gamma spectrometry was used to measure the activity of ^{210}Pb and ^{137}Cs on dried bulk sediment samples collected in the uppermost 35 cm of Oss17-1, with a Canberra GL2020R low-energy gamma detector at UMass Amherst. The ^{210}Pb profile was interpreted using the constant rate of supply (CRS) methodology (Appleby & Oldfield, 1978). Measurements of bulk lead obtained through XRF analysis was used to identify the onset of industrial Pb pollution (~1920) (Davis *et*

al., 1994). Cesium-137 is a globally distributed anthropogenic radionuclide introduced to the environment through nuclear weapons testing and is commonly used as an age marker in sediment cores (Zhang *et al.*, 2015). The onset of detectable ^{137}Cs corresponds to the year 1954 ± 1 , a result of high-yield nuclear testing beginning in 1952 and its subsequent atmospheric transport and fallout. The peak in ^{137}Cs correlates to 1963 ± 1 after nuclear weapons testing was banned in the atmosphere, outer space, and under water (Perkins & Thomas, 1980; Ritchie & McHenry, 1990; Walling, 2004; Cook *et al.* 2015; Zhang *et al.*, 2015).

Eleven radiocarbon samples were collected and sent to National Ocean Sciences Accelerator Mass Spectrometry laboratory at Woods Hole Oceanographic Institute in Woods Hole, Massachusetts and Direct AMS Radiocarbon Dating Service in Bothell, Washington, which both utilize accelerator mass spectrometry (AMS) techniques to obtain ^{14}C ages. Radiocarbon ages were calibrated to cal yr BP, utilizing the IntCal13 calibration curve in open sourced R software packages (Blaauw, 2010; Blaauw & Christen, 2011; Reimer *et al.*, 2013). The IntCal13 calibration curve relates radiocarbon years to calendar ages, and is specific to terrestrial samples in the northern hemisphere. Due to variations in atmospheric carbon isotope ratios through time, and its implications on ^{14}C calibration curves, the internal Gaussian distribution of uncertainty associated with measured ^{14}C ages is converted to a non-Gaussian distribution of uncertainty associated with calendar ages. Utilizing age-control points obtained through the above methods, different age-depth models were explored.

Age-depth models apply statistical approaches to estimate ages between age-control points and are essential for calculation of inferred watershed erosion rates. Linear accumulation rates (LARs), the rate at which sediment accumulates (cm/yr), were obtained directly from the

age-depth models. Mass accumulation rates (MARs) are the rate at which sediment accumulates per unit area ($\text{g}/\text{cm}^2/\text{yr}$) and were calculated using LARs:

$$MAR = \text{dry sediment bulk density} \times LAR \quad (1)$$

Clastic mass accumulation rates (cMARs) are the rate at which inorganic sediment accumulates per unit area ($\text{g}/\text{cm}^2/\text{yr}$):

$$cMAR = MAR \times (1 - LOI) \quad (2)$$

where LOI is in decimal form. I explored the implications of four different age-depth modelling techniques on calculations of cMARs because each technique applies a unique statistical approach to estimate ages and thus LARs.

Initially I used the ‘classical’ age-depth modelling package (CLAM) (Blaauw, 2010) in open-source R software (version 3.4.2). Linear interpolation and Monte Carlo simulations were applied to estimate thousands of possible LARs between age control points, in order to preserve the uncertainty associated with the age-control points. Estimated LARs obtained through each Monte Carlo simulation are assumed constant between age-control points. Within lakes LARs are however likely to vary, motivating the application of additional age-depth modelling techniques.

Bayesian accumulation statistics (Bacon) (Blaauw & Christen, 2011) were applied to two other age-depth models, also produced in open-sourced software R (version 3.4.2), and allows the user to force changes in LARs based on observed variations in stratigraphy. The Bacon model uses prior knowledge about sediment accumulation in lakes to produce more environmentally realistic estimates. An adaptive Markov Chain Monte Carlo approach is influenced by prior knowledge (accumulation rate) and coherence (memory) variables to

estimate millions of possible LARs at prescribed depth intervals between age-control points. The prior knowledge is controlled by the user and represents the estimated distribution of LARs through a gamma distribution around a mean estimated accumulation rate. Coherence represents the degree to which the accumulation rate for a particular section depends on the section above it. A low coherence is used when the accumulation rate is thought to have relatively large variations over time. The first age-depth model produced using Bacon techniques applied the default prior accumulation (acc.shape = 1.5, acc.mean = 20 yr/cm) and memory (mem.strength = 4, mem.mean = 0.7) over 5 cm depth intervals (146 total intervals) for the entire composite core. The second age-depth model produced using Bacon accounts for changes in LARs associated with the identified event layers by prescribing a change in sediment accumulation (acc.mean = 1 yr/cm) within the depths of the event layers, and uses the default prior accumulation (acc.mean = 20 yr/cm) outside the event layers. An accumulation mean of 1 yr/cm was used based on previous studies looking at event layers in sediment cores (Munoz *et al.*, 2010; Cook *et al.*, 2015). This model was constructed using 2 cm depth intervals (363 total intervals).

A ‘hybrid’ age-depth model was modified from the methods of Minderhoud *et al.* (2016) and allows for variations in accumulation rate between age-control points based on observations rather than interpretations. The time of sediment deposition at each cm (Δt) is determined as a function of the amount of time it takes for organic material to accumulate between age control points and the percent organic content at each cm:

$$\Delta t = LOI_i \times \frac{T_N}{\sum_{j=1}^N LOI_j} \quad (3)$$

where T_N is the amount of time between age-control points and i and j are individual sampled layers (1 cm). The age at each cm was then calculated as the age of the layer above plus Δt at

that cm. The primary difference in how ages were estimated in this study compared to Minderhoud *et al.* (2016) is they assume an exponential relationship between LOI and accumulation rate, whereas I assume a linear relationship.

3.3 Watershed analysis

Watershed geomorphic analysis using ArcGIS 10.2 provides an understanding of the spatial distribution of historic and modern processes that influence sediment transport and deposition within the Ossipee Lake watershed. Geomorphic analysis used 0.7 m and 1 m light detection and ranging (lidar) digital elevation models (DEMs) from NH Granit and 10 m DEMs from the U.S. Geological Survey (USGS). The Ossipee Lake drainage basin and its encompassing sub-drainage basins were defined using *StreamStats*, an online USGS application that uses 10 m DEMs to delineate user specified drainage areas.

To demonstrate the spatial extent of deforestation associated with EuroAmerican settlement within the Ossipee Lake watershed, lidar analysis was used to detect abandoned stone walls hidden beneath the present forest cover. Stone walls were commonly used by early EuroAmerican settlers to define the boundaries of agricultural and pasture land. Using previously established methods (Johnson & Ouimet, 2014), lidar DEMs were converted to hillshade and visually analyzed to detect linear features representing abandoned stone walls. The areas containing abandoned stone walls were compared to modern aerial photographs, collected in 2011, to highlight these lost artifacts of early colonization; however, this was not an exhaustive analysis of the entire watershed. Stone walls within the Ossipee Lake watershed and throughout New Hampshire can be further identified through the New Hampshire Department of Environmental Services (NHDES) crowd-sourced Stone Wall Mapping Project, which provides

an online lidar hillshade platform to explore the New Hampshire landscape with the goal of identifying these abandoned stone walls (NH Department of Environmental Services, 2019).

Longitudinal profiles of the major rivers and select tributaries within the Ossipee Lake watershed were constructed using lidar DEMs (Snyder, 2009). Channel centerlines were constructed in ArcGIS from mouth to headwaters, and converted to points with 0.7 to 1 m spacing to match the resolution of the lidar DEMs. Elevation values were extracted to the points to create a dataset of equally spaced distances from the river mouth and elevations.

Bed shear stress (τ_b) is a good proxy for sediment transport and was calculated at 100 m spaced survey points along channels (Snyder *et al.*, 2003):

$$\tau_b = \rho g n^{\frac{3}{5}} \left[\frac{Q}{w} \right]^{\frac{3}{5}} S^{\frac{7}{10}} \quad (4)$$

where channel gradient (S) was obtained from the longitudinal profiles, ρ is the density of water, g is the acceleration due to gravity, n is the channel roughness coefficient (0.04 based on Wilkins and Snyder, 2011), w is estimated bankfull channel width, and Q is discharge (Wilkins & Snyder, 2011). Channel width was determined empirically using a relation specific to New Hampshire streams (Schiff *et al.*, 2007):

$$w = 12.469A^{0.4892}. \quad (5)$$

Using a power-law relationship between discharge and drainage area (A), Q was estimated for each survey point along the channel (Wilkins & Snyder, 2011):

$$Q = k_q A^c \quad (6)$$

where k_q is an empirical, dimensionless coefficient representing discharge to the channel during an event with a specific recurrence interval and c is a constant dependent on the amount of the watershed that supplies water to the channel during a rainfall event and was assumed to be 1 (Dunne & Leopold, 1978; Wilkins & Snyder, 2011). Peak streamflow data from 1993 to 2017 collected at USGS gage station 01064801 in South Tamworth, NH (Fig. 3 A) was used to determine the Q with a 1.5 year recurrence interval (Q_{gs} , assumed to correspond to bankfull conditions), used to solve for k_q :

$$k_q = \frac{Q_{gs}}{A_{gs}} \quad (7)$$

where A_{gs} is the drainage area of the gage station.

4.0 Results

4.1 Subbottom sonar surveys

Subbottom sonar transects recorded ~20 m of unconsolidated sediment underlying the lake bottom based on instrument settings during data collection, and captured a prominent traceable reflection at ~7 m where data are sufficient (Fig. 11). At this reflection, less dense material overlays denser material, and the collected 8.63 m core penetrates through this reflection and recovered a portion of the underlying unit. Portions of the subbottom data had less successful imaging of the stratigraphy, likely due to the presence of gas within the sediment.

4.2 Core stratigraphy

The bottommost part of the southern basin composite core, below 6.895 m, is characterized as gray, diffuse lamina with black streaks (Fig. 12). Between depths of 6.895 to 5.74 m, sediment transitions into series of light brown and light gray intervals with black streaks

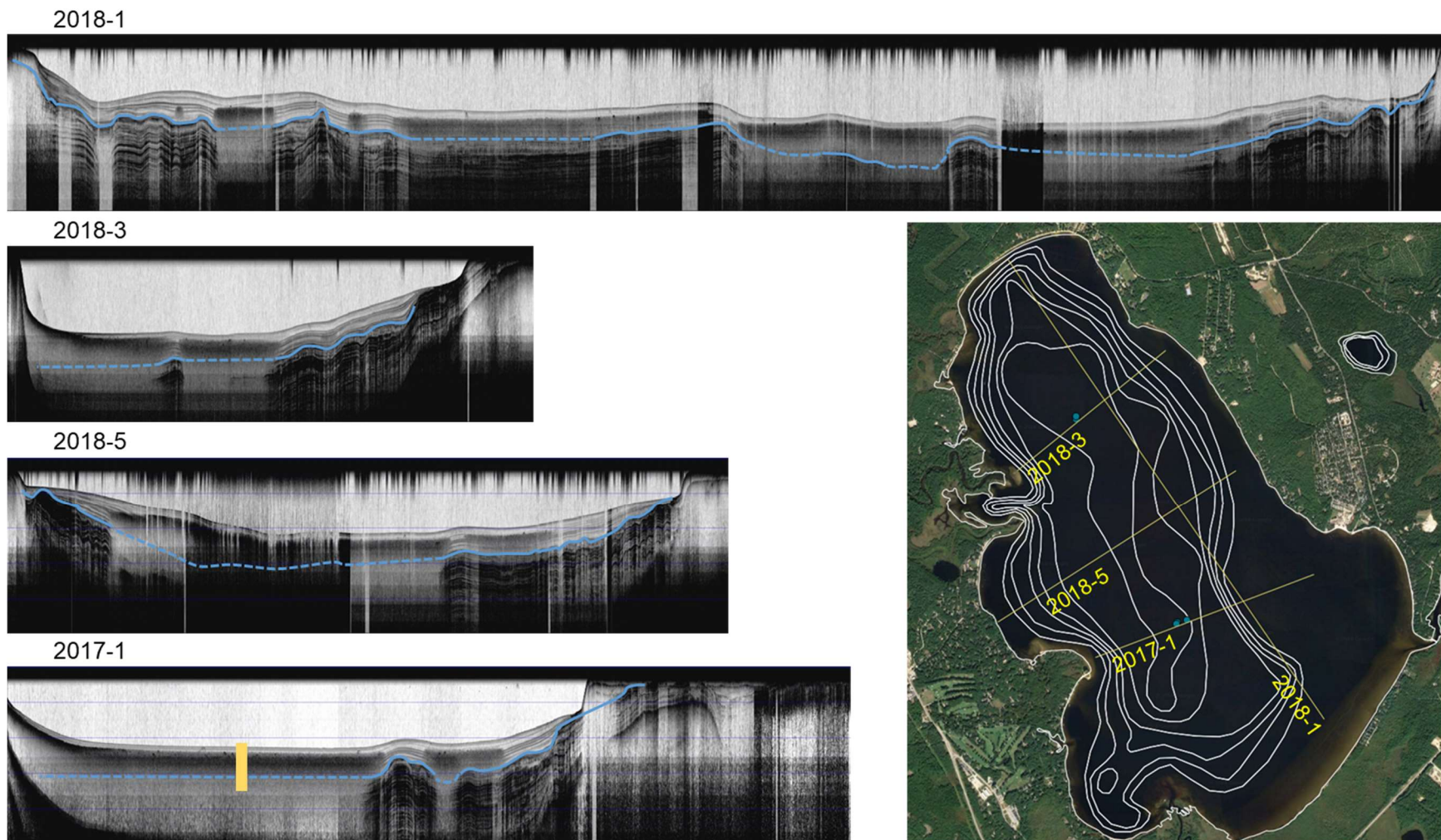


Figure 11. Subbottom sonar transects were collected approximately along the west-to-east and south-to-north tracks (yellow lines). Darker colors within the subbottom sonar transects represent a denser sediment compared to lighter colors. Transects were collected to provide insight to stratigraphic patterns observed within sediment cores (blue dots) compared basin-wide stratigraphy. Captured within all subbottom sonar transects is the transition (from bottom to top) of denser to less dense sediment. This transition is represented by solid blue lines in portions where there is clear imagery, and dashed blue lines where the image capture was less successful. The yellow rectangle in transect 2017-1 represents the approximate depth and location of the southern composite core.

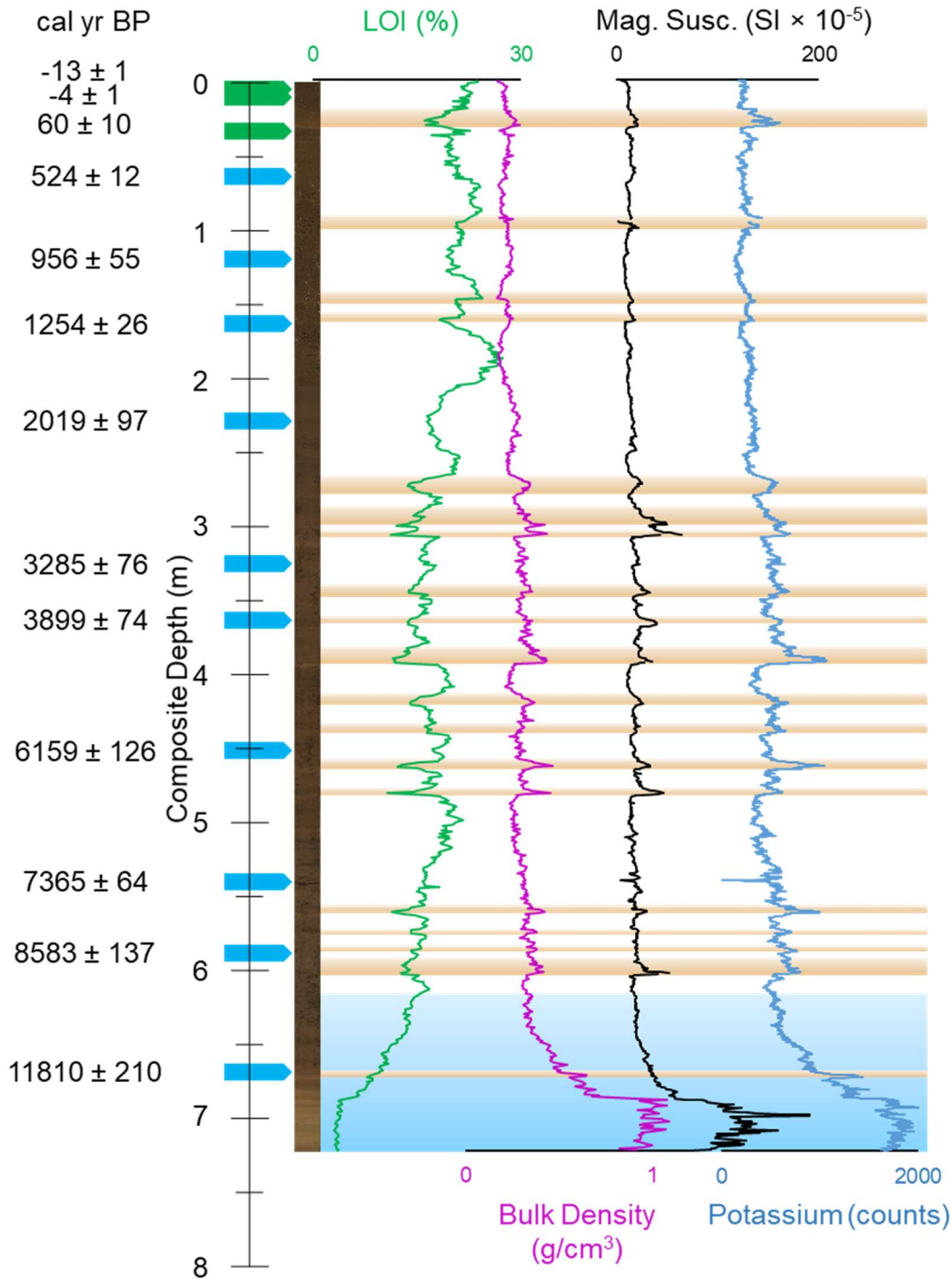


Figure 12. The southern basin composite core sequence from Ossipee Lake extends 7.25 m. Blue flags represent the depths at which samples were used for radiocarbon analysis, and green flags represent the depths of ^{137}Cs and ^{210}Pb age-control points (Tables 5, 6). Event layers (tan bands) are identified as sections of decreased organic sedimentation (LOI in green) and increased clastic sedimentation (bulk density in magenta, magnetic susceptibility in black, and K-counts in blue). The light blue band at the bottom of the core represents sedimentation prior to the Holocene and modern lake environment.

throughout, and above 5.74 m sediment is generally characterized as dark brown gyttja. Sediment below 6.895 m contains minimal organic content, LOI < 4.26 %. Between 6.895 and 5.74 m LOI increases to a maximum value of 16.78 %, and 27.43 % above 5.74 m. Dry bulk density below 6.895 m ranges from 0.82 to 1.09 g/cm³, decreases to 0.29 to 0.72 g/cm³ between 6.895 and 5.74 m, and further decreases to 0.17 to 0.46 g/cm³ above 5.74 m. Magnetic susceptibility below 6.695 m ranges from 17.08 to 191.24 SI × 10⁵ units, decreases to 13.32 to 69.58 SI × 10⁵ units between 6.895 to 5.74 m, and further decreases to 1.93 to 64.21 SI × 10⁵ units above 5.74 m.

Intervals of lighter brown sediment occur above 5.74 m of the composite record and are accompanied by a decrease in LOI with an increase in bulk density and magnetic susceptibility, and enriched K. This pattern was used to identify 19 irregularly-spaced event layers within the southern basin composite record ranging from thicknesses of 3 to 13 cm with an average thickness of 7.6 cm (Table 4; Fig. 12). Layers that follow the same geochemical pattern as the identified event layers but are less than 2 cm thick are rare and are not considered in this study.

The north basin composite core is composed primarily of dark brown, homogenous gyttja with magnetic susceptibility values that range from 0.61 to 26.06 SI × 10⁵ units (Fig. 13; Appendix). Both the north and south composite cores record a clastic event layer from 33.5 to 20 cm, shown through a transition to lighter brown sediment accompanied by increased magnetic susceptibility values. Grain size of sediment within all cores is too small to see with the naked eye. Similar patterns of magnetic susceptibility data are recorded in the north and south composite cores but at different depths (Fig. 13), suggesting changing vertical sedimentation rates. For instance, the double peak in magnetic susceptibility recorded between 1 and 1.2 m in the north composite core occurs between 1.4 and 1.6 m in the south composite core.

Table 4. Event layers identified in the south composite core record.

Event ID	Section core in composite sequence	Composite top depth (cm)	Composite bottom depth (cm)
1	17-2-1	20.5	33.5
2	17-2-2	91	100.5
3	17-2-2	144.5	152.5
4	17-2-2	157.5	163.5
5	18-2-1-2	267.5	280.5
6	18-2-1-2	290.5	302.5
7	18-2-1-2 into 18-1-2-1	305.5	309.5
8	18-1-2-1	340.5	348.5
9	18-1-2-1	364.5	369.5
10	18-1-2-1 into 18-2-2-1	383.5	394.5
11	18-2-2-1	417.5	425.5
12	18-2-2-1	437.5	443.5
13	18-2-2-1	460.5	467.5
14	18-2-2-1	478.5	483.5
15	18-2-2-1	559	565
16	18-2-2-1	575	578
17	18-2-2-1	587.5	591
18	18-2-2-1 into 18-1-3-1	595	606
19	18-1-3-1	671.5	676

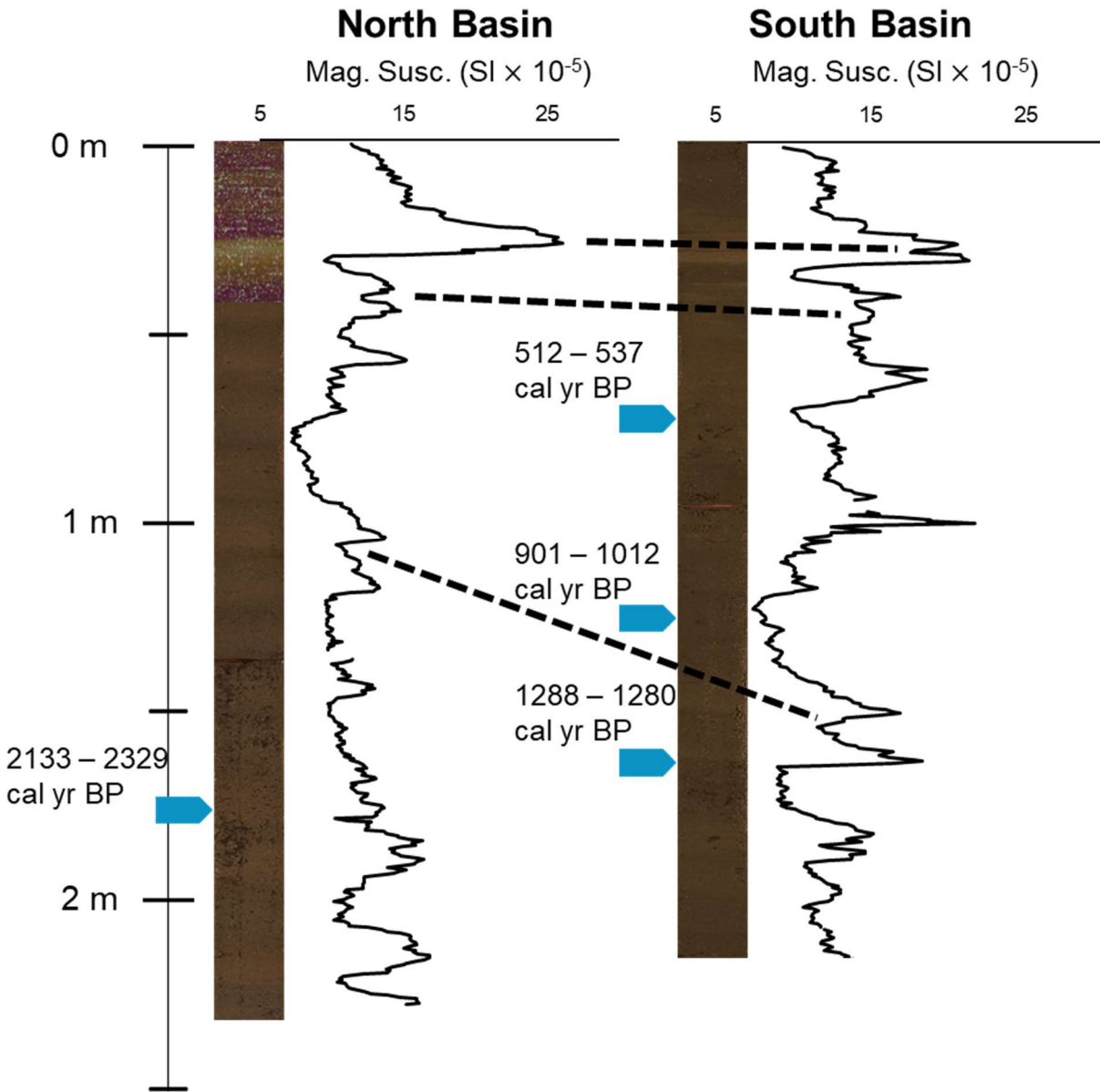


Figure 13. Core photographs and magnetic susceptibility measurements between the north and south basin composite cores were used to demonstrate the general agreement between sedimentation at both coring locations, providing evidence for basin-wide sedimentation events. Highest probability calibrated ^{14}C ages (cal yr BP) (Table 5) are marked with blue flags to the left of each core. Dashed lines correlate sections of the two cores that share similar patterns in magnetic susceptibility.

Table 5. Radiocarbon results all Ossipee Lake cores. Sample D-AMS 029670 was too small to obtain a ^{14}C age. Radiocarbon ages were calibrated using the IntCal13 calibration curve in open-source R using the CLAM package (Blaauw, 2010; Reimer *et al.*, 2013).

Lab ID	Material	Core	Section depth (cm)	^{14}C age	1 sigma error	Cal yr BP range	Prob. (%)
D-AMS 029670	Plant/Wood	17-2-1	72.5	500	15	512 - 537	95
D-AMS 029670	Plant/Wood	17-2-2	31	1030	45	800 - 814	2.5
						826 - 866	8.3
						901 - 1012	74.5
						1020 - 1056	9.6
D-AMS 029670	Plant/Wood	17-2-2	67	1290	15	1182 - 1209	36.6
						1228 - 1280	58.3
D-AMS 029670	Leaf fragments	18-2-1-2	37	2043	39	1902 - 1911	1.9
						1922 - 2116	93
D-AMS 029670	Pine needle	18-2-1-2	129	3069	29	3185 - 3186	0.3
						3209 - 3362	94.7
D-AMS 029670	twig	18-1-2-1	83.5	3574	33	3730 - 3745	2.4
						3768 - 3791	4
						3825 - 3974	88.6
D-AMS 029670	Small twig	18-2-2-1	80	<i>Insufficient material for analysis</i>			
D-AMS 029670	Bulk Sediment	18-2-2-1	84	5278	50	5933 - 6185	95
D-AMS 029670	Pine Needle	18-2-2-2	34	6450	38	7293 - 7299	1.4
						7301 - 7430	93.4
D-AMS 029670	Leaf fragments	18-1-3-1	21	7804	51	8446 - 8721	95
D-AMS 029670	Bulk Sediment	18-1-3-1	106	1012	48	11410 - 11431	1.2
				9		11479 - 11484	0.3
						11493 - 11551	3.9
						11600 - 12020	89.6
D-AMS 029670	Pine Needle	18-3-2	44	2208	40	2133 - 2329	95

I focused geochronological analyses on the longer record obtained in the southern basin, and present the results in greater detail in section 4.3. Northern composite record ages were estimated through linear interpolation between the core surface (-67 cal yr BP) and the calibrated radiocarbon age obtained from composite core depth 181 cm (2231 cal yr BP; Table 5). The radiocarbon age from the northern composite record is generally younger than those obtained from the southern composite record (Fig. 13). The estimated LAR in the northern composite record above the ^{14}C age-control point (181 cm; Table 5) is 0.08 cm/yr, and the average LAR in the southern composite record above 180 cm is 0.14 cm/yr.

4.3 South basin core chronology

Gamma spectrometry analysis identifies the onset and peak of ^{137}Cs at 14.5 cm and 11.5 cm, respectively, which correspond well with estimated ages produced through the ^{210}Pb model (Fig. 14 A; Table 6). The general agreement between estimated ages obtained through ^{137}Cs and ^{210}Pb (Fig. 14 A & C) in this uppermost section of the southern composite core suggests the CRS model provides a reasonable approximation of ages over this interval. Uncertainties in the ^{210}Pb model increase with depth, making the bottommost portion of the record, below ~20 cm, more difficult to interpret. The ^{210}Pb model estimates the age of the uppermost event layer, from 33.5 to 20.5 cm (Event ID 1; Table 4), to be ~ 80 cal yr BP (1870). If Event ID 1 were to occur at the estimated age obtained through the ^{210}Pb age-depth model, sediment accumulation within the event layer would have to be lower than the section above it, which is well constrained. Therefore, the uppermost event layer would have to be more recent than suggested by the ^{210}Pb model. Further insight to chronology is provided by measurements of bulk Pb obtained during XRF analysis (Fig. 14 D). Bulk Pb begins to increase above ~27 to 28 cm and can be attributed to the addition and burning of Pb in gasoline during the 1920s (Luce, 2012). Event ID 1 must

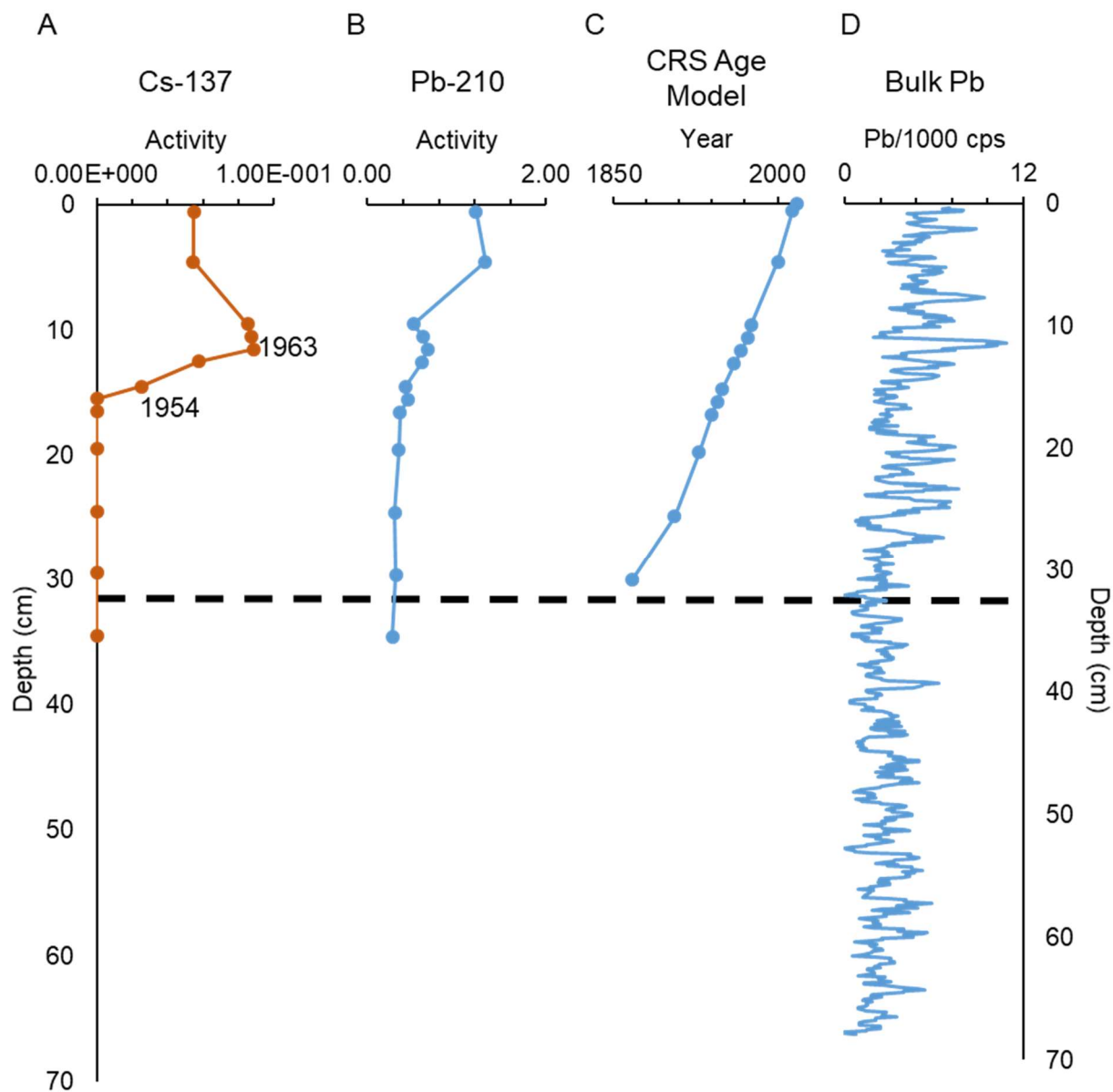


Figure 14. Cesium-137 (A) and lead-210 (B) activity profiles obtained through gamma spectrometry. The ages labeled on the ^{137}Cs profile correspond to the onset and peak in ^{137}Cs . The constant rate of supply method was used to construct the ^{210}Pb age-depth model (C) because estimated ages using this technique agree within a few years of the onset and peak in ^{137}Cs . (D) Bulk lead counts from XRF analysis over a 0.5 cm moving average shows an increase ~27 to 28 cm. The dashed horizontal line represents the uppermost event layer (bottom depth 33.5 cm) used to help guide chronologic analysis.

Table 6. Age-control points used to construct age-depth models of the south composite core record, with reported uncalibrated ^{14}C ages. *The inferred age-control point is at the base of the uppermost event layer (Event ID 1 on Table 4)

Sample	Core	Section depth (cm)	Composite depth (cm)	Age (cal yr BP)	Age (^{14}C age)	1 sigma error
Surface	17-2-1	0	0	-67		1
^{137}Cs peak	17-1	11.5	11.5	-13		1
^{137}Cs onset	17-1	14.5	14.5	-4		1
Inferred*	17-2-1	33.5	33.5	60		10
^{14}C	17-2-1	72.5	72.5		500	15
^{14}C	17-2-2	31	127		1030	45
^{14}C	17-2-2	67	163		1290	15
^{14}C	18-2-1-2	37	237		2043	39
^{14}C	18-2-1-2	129	329		3069	29
^{14}C	18-1-2-1	83.5	371.5		3574	33
^{14}C	18-2-2-1	84	457		5278	50
^{14}C	18-2-2-2	34	546		6450	38
^{14}C	18-1-3-1	21	595		7804	51
^{14}C	18-1-3-1	106	680		10129	48

therefore occur between 80 and 30 cal yr BP (1870 and 1920), and was inferred to begin at 60 ± 10 cal yr BP (1890 ± 10 ; years; Table 6).

The oldest dated ^{14}C sample is 10129 ± 48 ^{14}C age (11810 ± 210 cal yr BP) taken from a bulk sediment sample at composite depth of 680 cm (Tables 5 and 6). There are no reversals in the radiocarbon age sequence, and the age-depth models depict varying rates of sediment accumulation throughout the record. The estimated age of the record (to the bottom of the core at 7.25 m) is 11143 to 13803 cal yr BP depending on the modelling technique applied (Fig. 15). Estimated ages between the different modelling techniques vary the most below 6 m, where age-control points are limited and LARs likely changed rapidly in response to deglaciation. The CLAM (Fig. 15 A) and Bacon without event layers (Fig. 15 C) models produce estimated ages most similar to each other compared to the other modelling techniques, with a maximum difference in age between these two models of 289 years at 679.5 cm depth and an average difference in estimated ages of 35 years for the entire record. The Bacon that considers event layers (Fig. 15 D) and the hybrid model (Fig. 15 B) showed greatest variation in estimated ages, with a maximum difference in estimated ages of 798 years at 662.5 cm and average age difference of 100 years for the entire record.

Peaks in LARs vary widely according to the treatment of sedimentation within event layers among the different age-depth modelling techniques (Fig. 16). The CLAM and Bacon without event layers models do not account for changes in sedimentation rate associated with event layers and do not produce LARs within event layers that differ from sedimentation outside event layers. The Bacon model that accounts for variations in sedimentation rate associated with event layers (horizontal dotted lines in Fig. 15 D) produces much higher LARs (up to 1 cm/yr) within event layers, which is strongly influenced by the somewhat arbitrarily assigned prior

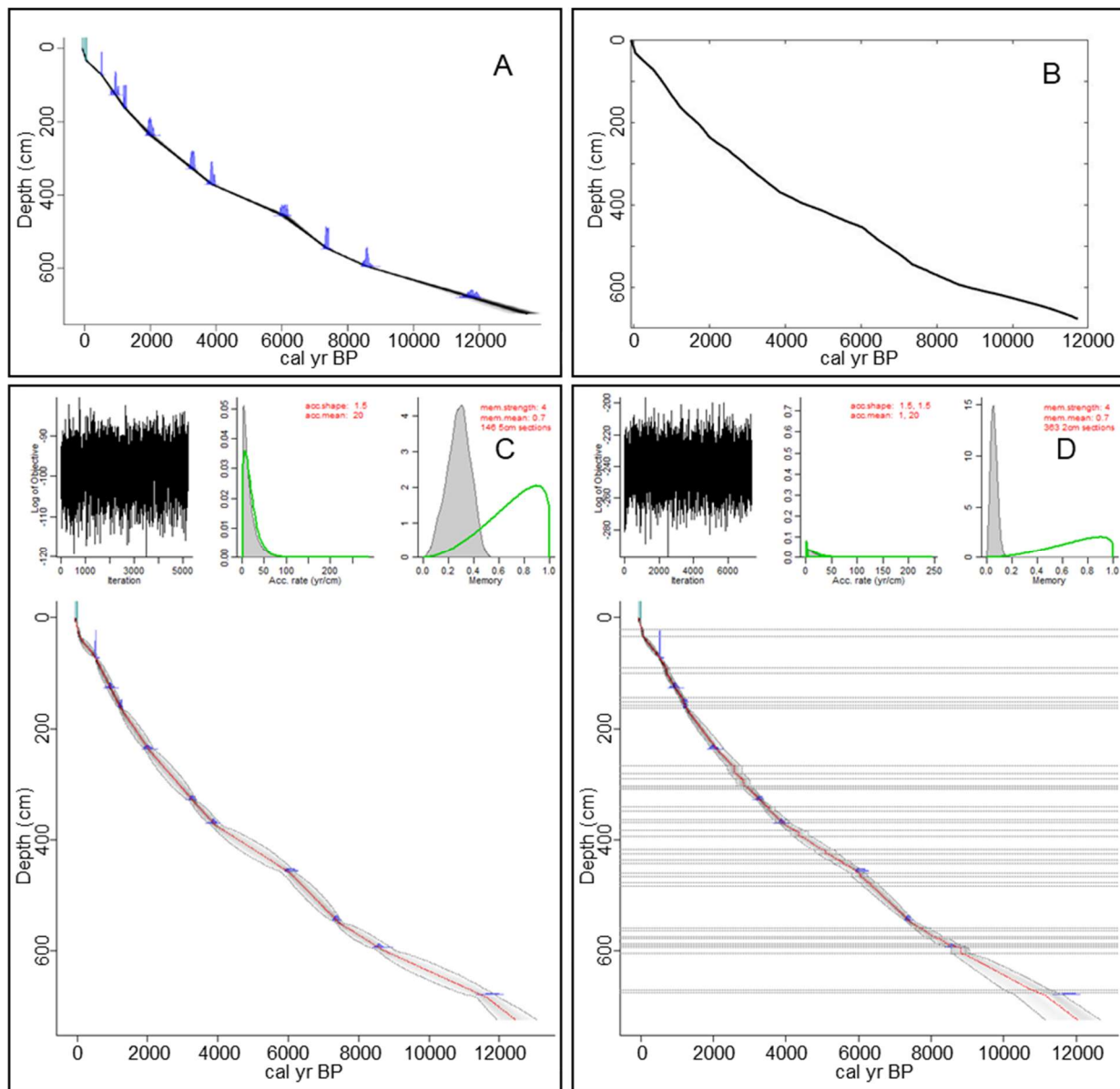


Figure 15. Age-depth models were constructed through the application of various statistical approaches. Using CLAM in R software (A), linear interpolation assumes constant sediment LARs between age-control points (Blaauw, 2010), whereas using a hybrid age-depth model (B), the estimated LARs obtained through linear interpolation vary between age-control points as a function of LOI (Minderhoud *et al.*, 2016). Bacon, applied in R software, (C, D) allows for variations in sedimentation between age-control points as a function of prior estimates on LARs and coherence. Age-depth model C uses the default accumulation and memory priors in Bacon (acc.shape = 1.5, acc.mean = 20 yr/cm, mem.strength = 4, mem.mean = 0.7) within 5 cm depth intervals over the entire core. Variations in sediment accumulation within event layers were considered in age-depth model D by using the default priors in non-event lake sedimentation and changing priors within the event layers (acc.shape = 1.5, acc.mean = 1 yr/cm, mem.strength = 4, mem.mean = 0.7) over 2 cm depth intervals.

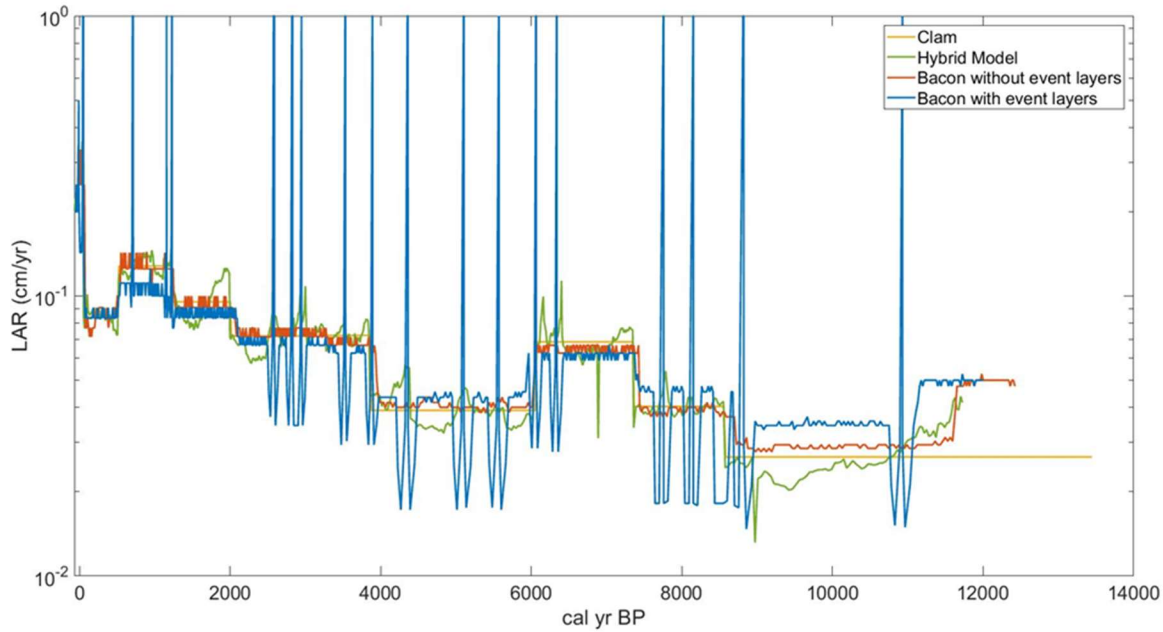


Figure 16. Linear accumulation rates (LARs) for each age-depth modelling technique from Fig. 15 represent the rate at which vertical sedimentation occurs and was modelled every cm. Using linear accumulation through CLAM, LARs are constant between age-control points with sharp changes in LAR occurring at the depths of age-control points. The Bacon models also produce sharp changes in LAR at the depths of age-control points but produce additional small fluctuations in LAR between age-control points. Spikes in LAR associated with event layers using the Bacon model that considers event layers reach the prior estimated mean accumulation rate (1 yr/cm) and produce dips in LAR immediately before and after event layers. The hybrid model produces the largest variations in LAR between age-control points, driven by changes in the organic content of sediment.

accumulation mean, which is constrained by a general understanding of lake sedimentation. This Bacon model produces dips in LAR before and after event layers, and are a relic of the numerical techniques of the model. The hybrid age-depth model produces LARs within some event layers that are elevated compared to the CLAM and Bacon without event layer models, but not to the extreme of the Bacon with event layers (Fig. 16). The changes in sedimentation produced within the event layers through the hybrid model are driven by variations in LOI, used as a proxy of organic versus clastic accumulation within the lake.

Calculated clastic mass accumulation rates (cMARs) provide greater high frequency variation in sediment accumulation relative to LARs by incorporating LOI and dry bulk density data at cm scale resolution. Above the bottommost age-control point (680 cm), cMARs generally agree among the different age-depth models (Fig. 17). Bacon considering event layers produces both the minimum and maximum cMAR (Table 7). Troughs in cMAR are produced immediately before and after event layers similar to those observed in LARs. The highest peaks in cMAR between all applied modelling techniques occur within the event layers in the Bacon model that accounts for changes in sedimentation associated with event layers.

Clastic mass accumulation rates vary throughout the record regardless of the age-depth model applied. Overall cMAR has a slightly increasing linear trend following deglaciation, at a rate of $0.002 \text{ g/cm}^2/\text{yr}$ per 1000 years and an R^2 between 0.286 to 0.348 (Fig. 17). This increasing linear trend is not observed in the Bacon with event layers model. Periods of elevated cMAR occur ~8500 to 7800, ~6500 to 2500, and 1600 cal yr BP to present. Event layers occur relatively infrequently with up to 0.6 events per century occurring 2868 to 2774 and 997 to 987 cal yr BP (Fig. 18 B). The minimum duration between event layers is 88 years and the maximum duration is 2593 years, with an average of 614 years between event layers. Periods of elevated

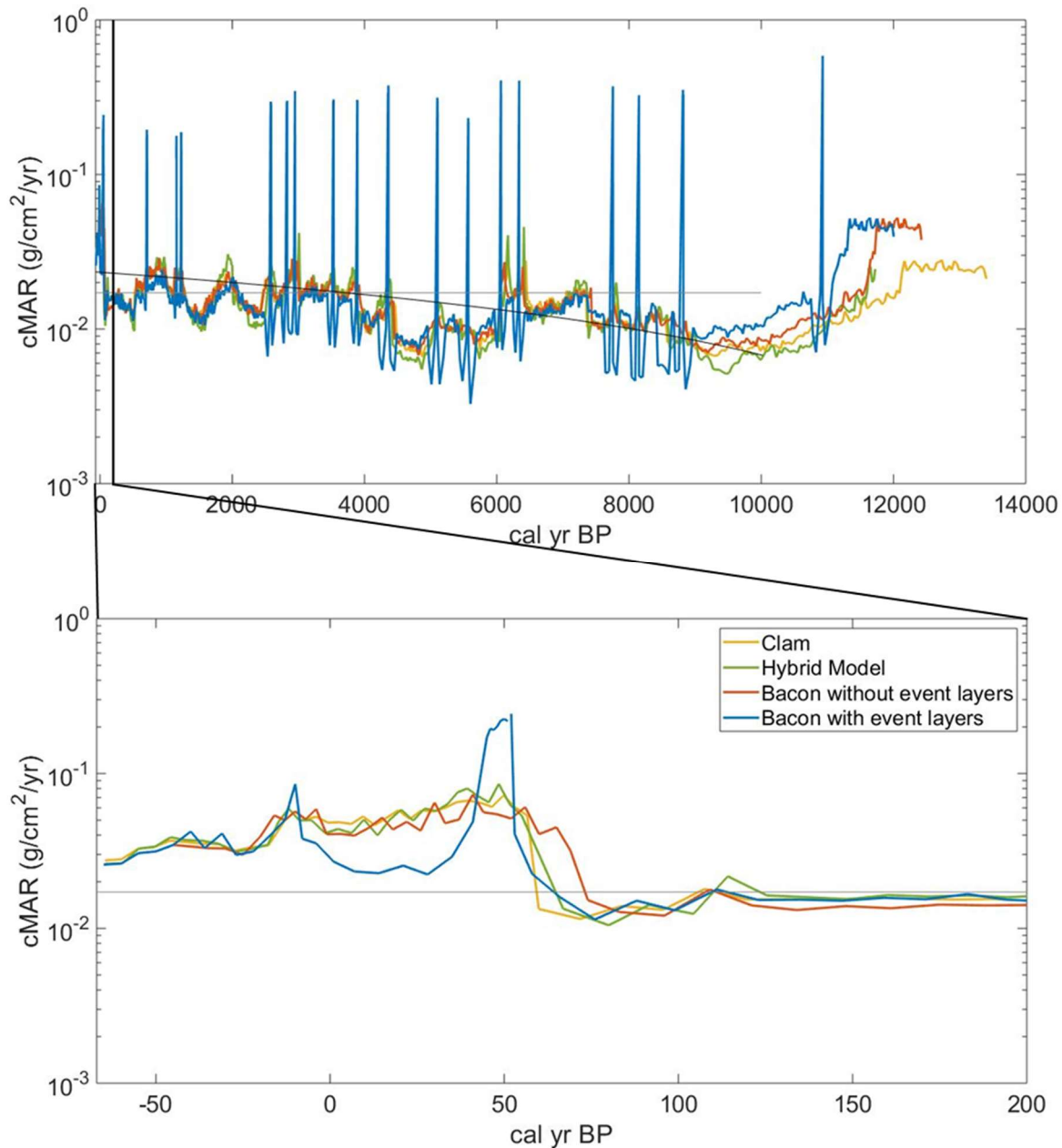


Figure 17. Clastic mass accumulation rates serve as a proxy for watershed erosion rates, and variations in cMAR between the age-depth modelling techniques highlight the influence of different age-depth models on accumulation rates. The gray horizontal line represents the mean cMAR value over the past 10,000 years, the portion of the record above the bottommost age-control point. Mean cMAR values from the Bacon without event layers and hybrid models agree within the same order of magnitude of that produced by the CLAM model, however the mean cMAR from the Bacon with event layers is two orders of magnitude greater. The linear trend line over the past 10,000 years (black diagonal) was constructed using the CLAM model, and the Bacon without event layers and hybrid models produce very similar trends.

Table 7. Mean, minimum, and maximum cMARs ($\text{g}/\text{cm}^2/\text{yr}$) between the applied age-depth modeling techniques provide insight to how different statistical approaches influence accumulation rates.

Age-depth model	Panel in Figure 15	Mean cMAR	Minimum cMAR	Maximum cMAR
CLAM	A	0.017	0.0066	0.072
Bacon without event layers	B	0.018	0.0068	0.073
Bacon with event layers	C	0.048	0.0033	0.587
Hybrid	D	0.017	0.0051	0.086

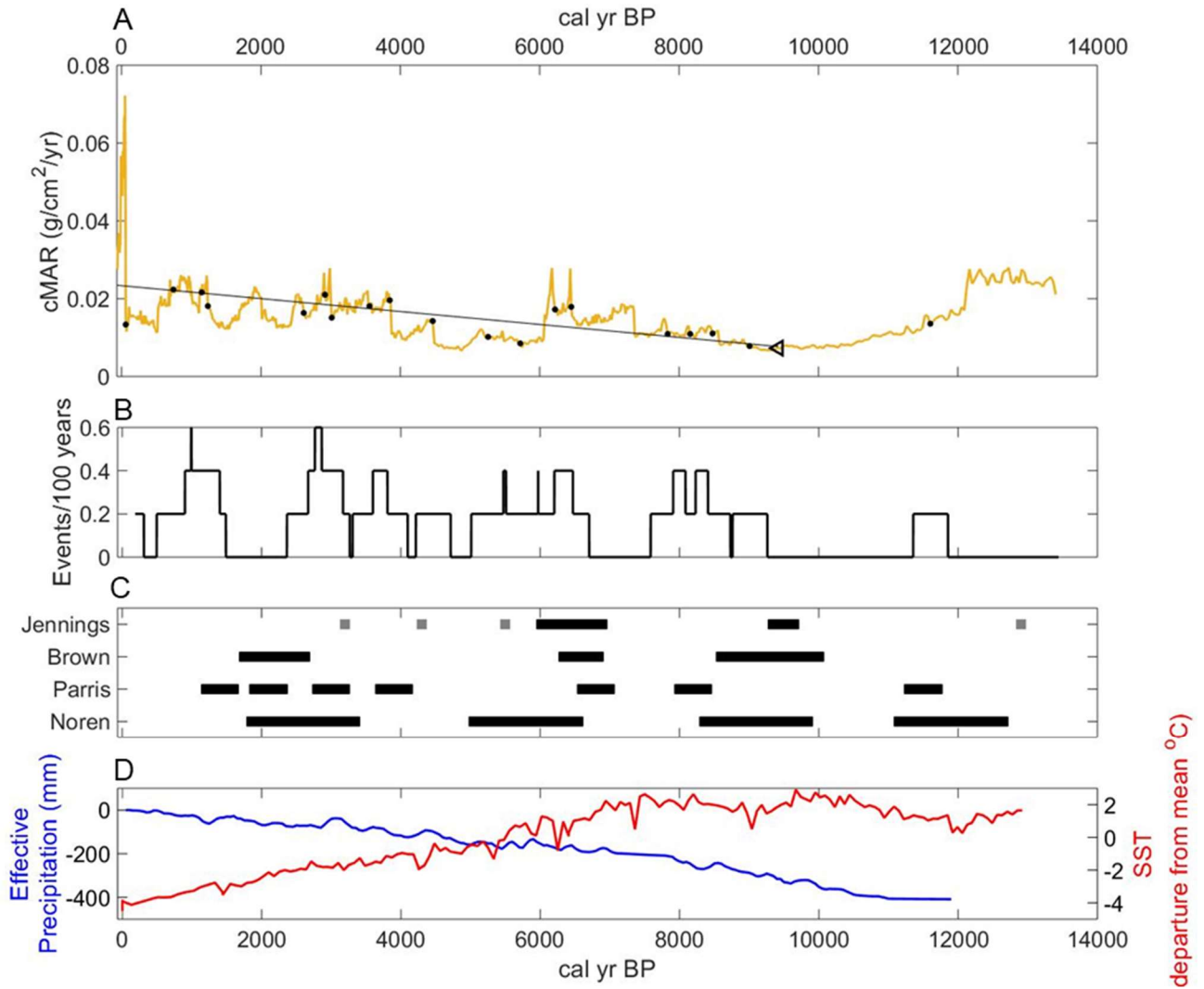


Figure 18. (A) Clastic mass accumulation rates using estimated ages produced from the CLAM age-depth model (Fig. 15 A) with black dots representing the onset of event layers. The black triangle represents the transition into the Holocene lake environment (~9400 cal yr BP, 617 cm; Figs. 12 and 15) and the black line represents increasing cMAR following the transition ($R^2 = 0.2498$ and $m = 1.6611$). (B) Ossipee Lake event layer frequency over a 500 year sliding window based on estimated ages using CLAM (Fig. 15 A). Up to 0.6 events per 100 years are observed from 2868 to 2774 and 997 to 987 cal yr BP. (C) Other post-glacial records of New England sedimentation (Brown *et al.*, 2000; Noren *et al.*, 2002; Jennings *et al.*, 2003; Parris *et al.*, 2010). Black bars represent periods of increased sedimentation and gray bars represent periods of soil development.

cMAR correspond to periods of more frequent event layers except over the past ~150 years where cMAR values are elevated but event frequency is relatively low (Figs. 17 and 18).

4.4 Ossipee Lake watershed

Lidar analysis capable of detecting fine-scale topography reveals abandoned stone walls hidden under the presently forested landscape (Fig. 19). Stone walls were primarily identified in the southern portion of the Ossipee Lake watershed near the upstream reaches of the Pine River (Fig. 19). Initial results from the NHDES Stone Wall Mapping Project show a similar pattern, with the majority of stone walls in the southern and northeastern portion of the watershed (NH Department of Environmental Services, 2019). Stone wall analysis was performed on ~ 5 % of the entire watershed. Stone walls were identified in ~ 1 % of the Ossipee Lake watershed, less than the more exhaustive study by Johnson & Ouimet (2014) who discovered new archeological sites in just over 5 % of their study area. The presence of stone walls supports the presence of EuroAmerican settlement within the Ossipee Lake watershed.

Longitudinal profiles highlight variations in channel gradient associated with the Lovell, Pine, and Bearcamp rivers (Fig. 7). The Pine River is a relatively low gradient river (ranging in elevation from 123 to 175 m) compared to the Lovell (123 to 576 m) and Bearcamp River with its Cold and Swift river tributaries (123 to 638 m). Since τ_b is strongly dependent on channel slope (Equation 4; Snyder *et al.*, 2003), the Pine River has lower τ_b (mean = 18.5 Pa, standard deviation = 12.8 Pa) compared to the Lovell (mean = 83.6 Pa, standard deviation = 41.5 Pa) and Bearcamp (mean = 28.6 Pa, standard deviation = 31.6 Pa) rivers with its Cold (mean = 71.9 Pa, standard deviation = 44.4 Pa) and Swift (mean = 76.4 Pa, standard deviation = 28.1 Pa) river tributaries. The higher gradient Lovell, Cold, and Swift rivers have relatively high τ_b values throughout the channel.

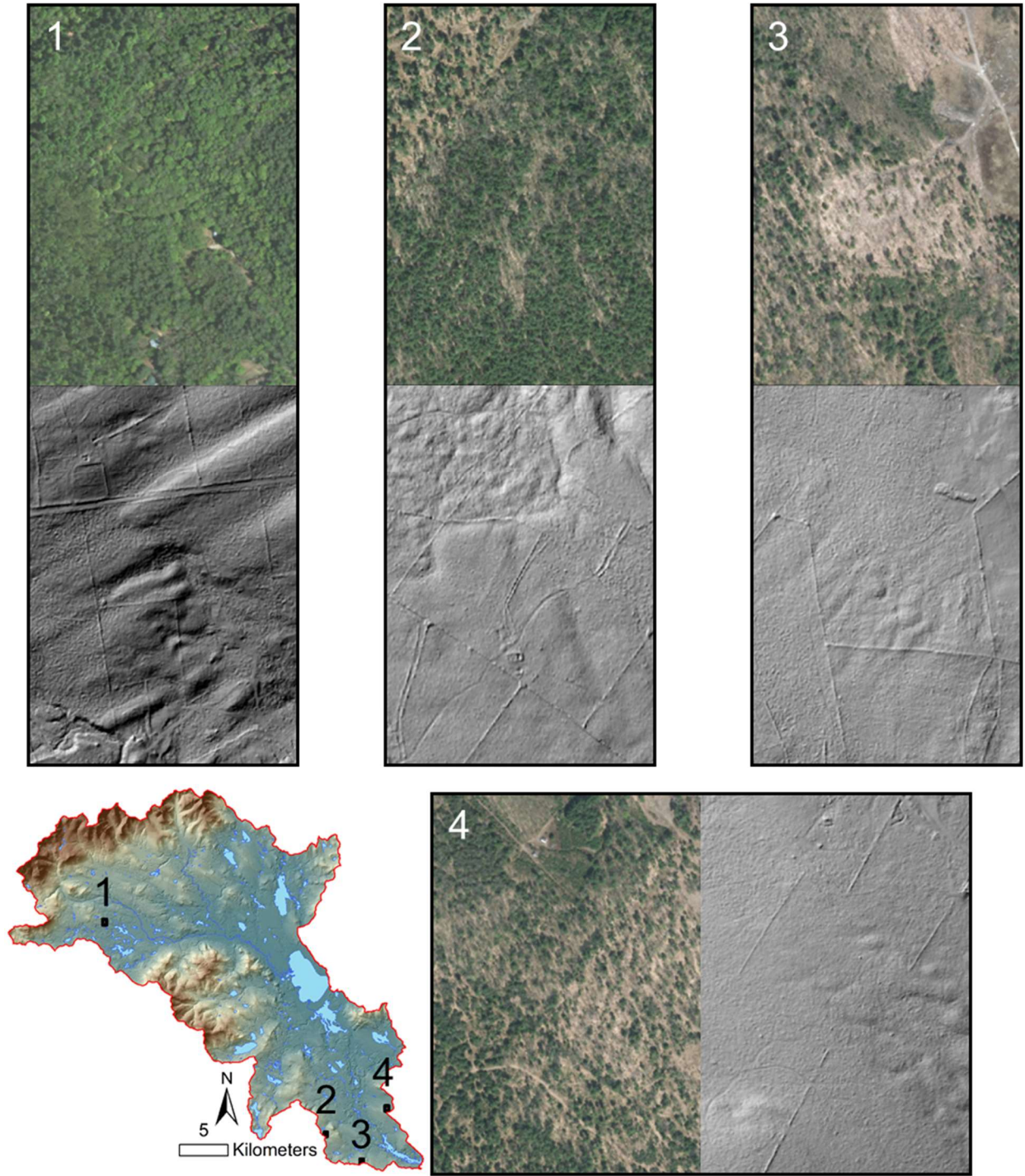


Figure 19. Lidar hillshade images (right) capture abandoned stonewalls hidden under the current forest cover (left) and provide evidence for clear-cut landscapes within the Ossipee Lake watershed during the period of European settlement.

5.0 Discussion

5.1 Sediment supply from the watershed to Ossipee Lake

Bed shear stress (τ_b) analyses provide insight to areas that can serve as sources of sediment and areas that act as sinks. The relatively larger τ_b within the Lovell and Bearcamp rivers with the Cold and Swift river tributaries have higher sediment transport capacities (Fig. 7) compared to the Pine River. The lower reaches of the Bearcamp and Lovell rivers just upstream of Ossipee Lake have low τ_b and likely represent depositional zones. These areas can potentially trap mobilized sediment, and limit sediment delivery to Ossipee Lake under certain flow conditions. Bed shear stress data therefore highlights the importance of the upstream reaches of the Lovell and Bearcamp rivers as areas of sediment transport, with the downstream reaches of these rivers and the Pine River serving as potential sediment sinks.

The supply of sediment to these rivers is also important when evaluating the ability of these rivers to deliver sediment to Ossipee Lake. The surficial geology surrounding the Lovell River is primarily thin till on bedrock (Fig. 2) within the Ossipee Mountains. The middle-reaches of the Bearcamp River and the lower-stretches of the Cold and Swift rivers are in areas of stratified outwash deposits consisting of gravel, sand, and silt. The outwash deposits are a more easily mobilized material compared to the till that dominates the Lovell River watershed, resulting in incised valleys into the deposits. The Bearcamp River has more incision (up to ~ 40 m) compared to the Lovell River (up to ~ 30 m), and the Bearcamp River is able to carve valleys over a relatively greater distance, shown by the expansive proglacial deposits surrounding the Bearcamp River compared to the predominance of thin till surrounding the upstream reaches of the Lovell River (Fig. 2). Even though the Bearcamp River and tributaries are believed to be the primary supplier of sediment to Ossipee Lake, the ability of the Lovell River to transport finer

sediment derived from upland till should not be discredited, especially considering the dominance of fine sediment within the cores. The relative sediment transport capabilities of the channels described above is further evidenced by the characteristics of the river channels themselves. The banks in lower stretches of the Pine River are well vegetated and relatively stable, whereas the lower stretches of the Bearcamp River contain bare sandbars indicating active sediment transport.

The relative understanding of how these rivers supply sediment to Ossipee Lake influenced coring locations. The deltas present at the mouths of the three major rivers suggest sediment is being delivered to Ossipee Lake from the watershed. The Bearcamp River likely has the most active delta due to its relatively high sediment transport capabilities (Fig. 7) and sediment supply (Fig. 2). These deltas can cause localized changes in lake sedimentation, such as delta progradation or slumps. To ensure changes in sediment properties recorded in Ossipee Lake cores are not sourced from reworked sediment via inner-lake dynamics, cores were compared from multiple locations and the long composite core was collected from in a distal location in the southern part of the lake 1.89 km from the Bearcamp River delta.

5.2 Age-depth models

Age-depth models can have strong implications on results, and it is important to understand how the models estimate ages and influence LARs. Multiple age-depth modelling techniques were applied in this study to explore how different statistical techniques influence cMAR, a function of LAR, dry bulk sediment density, and LOI (Equation 2). Clastic mass accumulation rates (cMARs) produced using the CLAM and Bacon without events underrepresent changes in cMAR associated with event layers (Fig. 17) by not allowing for variations in LAR between predefined age-control points. The Bacon model that considers

changes in sedimentation associated with event layers allows for larger variations in cMAR within event layers. The magnitude of these changes in sedimentation are strongly influenced by the estimated prior terms, and determination of prior terms is difficult (Trachsel & Telford, 2017). Identifying the depths of event layers is largely subjective, and can vary from user to user. Another especially difficult challenge is estimating LARs within event layers, where sediment grades upwards to gyttja suggesting LAR is not constant within the event layers themselves. No data exist within the Ossipee Lake record that provides insight to the duration of event layers. The purely statistical approaches used in estimating LARs, in addition to the subjectivity associated with assigning prior conditions, are major limitations of the age-depth models discussed above. The hybrid age-depth model was explored because LARs are able to vary as a function of sediment properties, so the model produces spikes in cMAR within event layers without the subjectivity of defining the depths and estimated LARs of event layers.

Duration of event layers estimated through the various age-depth models range from 19 to 676 years depending on the model (Table 8), suggesting clastic sedimentation remains elevated following an initial disturbance to the landscape. Prolonged elevated sedimentation is also observed in Amherst Lake, VT, however, event layer durations in Amherst Lake do not exceed 80 years (Cook *et al.*, 2015). Additionally, rapid channel recovery (1 to 2 years) has been observed in New England rivers (Renshaw *et al.*, 2019). The relatively long duration of event layers in Ossipee Lake compared to Amherst Lake (Cook *et al.*, 2015) and rapid channel recovery (Renshaw *et al.*, 2019) suggest the decadal- to centennial-scale duration of event layers produced through the Ossipee Lake age-depth models potentially underrepresent changes in LARs and cMARs within event layers. The relatively long duration of event layers also highlights the difficulty in representing LARs within event layers. While the hybrid age-depth

Table 8. Estimated duration of event layers within the south composite record.

Event ID	Composite top depth (cm)	Composite bottom depth (cm)	CLAM duration (years)	Hybrid duration (years)	Bacon without event layers duration (years)	Bacon with event layers duration (years)
1	20.5	33.5	43.7	49.8	51	31
2	91	100.5	70.4	69.6	70	19
3	144.5	152.5	62.5	63.2	63	30
4	157.5	163.5	48.3	47.7	49	30
5	267.5	280.5	180.6	163.7	179	41
6	290.5	302.5	166.7	145.8	161	68
7	305.5	309.5	55.6	47.1	54	61
8	340.5	348.5	110.6	104.7	115	73
9	364.5	369.5	69.1	62.2	74	55
10	383.5	394.5	282	215.1	273	165
11	417.5	425.5	205.1	183.1	201	133
12	437.5	443.5	153.8	159.3	143	130
13	460.5	467.5	102.1	83.2	109	58
14	478.5	483.5	72.9	60.3	79	57
15	559	565	148.9	129.2	159	114
16	575	578	74.5	71.8	75	57
17	587.5	591	74.4	70.6	75	165
18	595	606	394.3	437.3	321	67
19	671.5	676	150.2	98.6	136	149

model helps to eliminate a level of subjectivity in assigning prior conditions and depths of event layers, spikes in cMARs within event layers are only slightly larger than those produced using CLAM. The nonexistence of spikes in cMAR within event layers that exceed the bacon with event layers model suggests the hybrid model still likely underrepresents accumulation associated with event layers. Further application of the hybrid model should apply an exponential relationship between LOI and sedimentation (Minderhoud *et al.*, 2016) to explore the influence of this relationship and potentially produce larger spikes in cMAR.

It is important to consider that in this study calculations based on the age-depth models, such as cMAR, are based on the median or highest probability age, and do not account for the uncertainties in the age-control points used to create the models. The reported LAR and cMAR values (Figs. 16 and 17) represent the highest probability values, but lack propagated errors or probabilities of other values, producing the most likely, but overly confident results.

5.3 Spatial variations in sedimentation within Ossipee Lake

To evaluate whether sedimentation recorded in the southern composite record represents basin-wide variations, properties (magnetic susceptibility and estimated ages) between the north and south basin composite cores (Fig. 1 B) are compared. Changes in magnetic susceptibility can be correlated among the two cores, but occur at different depths within the cores (Fig. 13). Below ~ 0.75 m, similar patterns in magnetic susceptibility occur at deeper depths in the southern composite record, as shown by the similar double peaks around 1.1 m and 1.5 m in the north and south composite cores, respectively. Furthermore, the four cores analyzed from different locations in Ossipee Lake by Perello (2015), in addition to the two composite cores analyzed in this thesis, all record the same event layer at 33.5 cm (Event ID 1; Table 4). The

similar relative patterns of magnetic susceptibility and presence of the event layer at 33.5 cm in multiple cores suggest sediment deposition occurs basin wide but at different rates.

The younger calibrated ^{14}C ages and greater LARs in the southern record suggest overall accumulation rate in the southern composite record is greater. The greater LAR observed in the southern composite core is consistent with characteristics of the lake and watershed. The net littoral transport within Ossipee Lake is in the southeastward direction, indicated by the sandy shelf extended from the southeast corner of Ossipee Lake (Figs. 1 B and 5; Newell, 1960; Newton, 1974a). Additionally, the southern coring location is closer to the Lovell and Bearcamp River inlets, providing larger quantities of sediment to the southern part of the lake.

Qualitative observations of grain size in the cores further support the interpretation that spatial variations in sedimentation are driven by external forces rather than inner-lake dynamics. The fine grain size within event layers suggests sediment was deposited from suspension, whereas coarser sediment would imply transport through density driven currents along the lake bottom that could be driven by slumping of the delta slope.

While the evidence above suggests variability recorded in the south basin is broadly representative of sedimentation across the entire lake basin, additional analyses could further confirm or refute interpreted basin-wide sedimentation. Measurements of LOI, bulk density, K counts, and grain size from both cores are required to further understand basin wide variations in LARs. Additional insight can be obtained through added ^{14}C analysis on the northern composite core. High resolution bathymetry and subbottom surveys could also provide potential insight on pathways and mechanisms of sediment transport (Normandeau *et al.*, 2016).

5.4 Paraglacial sedimentation

Below 6.895 m in the south basin composite core, sediment is predominantly clastic with minimal organic content (LOI between 3.2 to 6.6 %; Fig. 12), and is accompanied by the highest prolonged cMARs in the record (0.03 to 0.05 g/cm²/yr; Fig. 17). During this period, the present Ossipee Lake may have been a part of the larger Glacial Lake Ossipee (Newton, 1974a; Medalie & Moore, 1995; Moore & Medalie, 1995). From 6.895 to 6.175 m, the sediment gradually transitions into the more typical modern gyttja, as shown through a change in sediment color, increase in LOI (range of 4.1 to 15.4 %), and decrease in clastic proxies (Fig. 12). This interval likely represents the transition to a post-glacial environment following ice retreat as vegetation began to establish itself. This transition is further observed in subbottom sonar surveys of Ossipee Lake, where a contact between acoustically denser sediment and less dense sediment occurs at approximately the same depth (Fig. 11).

The timing of deglaciation within the Ossipee Lake watershed is difficult to link to the timing of reconstructed ice retreat in this part of New England 14500 cal yr BP (Ridge *et al.*, 2012) due to poorly constrained ages below 6.8 m in the cores. A basal ¹⁴C age collected at depth 6.8 m (Table 5) corresponds to 11810 ± 210 cal yr BP. The timing of this basal age relates well to the drainage of glacial Lake Pigwacket, a series of glacial lakes in the White Mountains from 12170 to 11630 cal yr BP (Shuman *et al.*, 2005), but is younger than basal dates from other lakes surrounding the White Mountain region including Echo Lake, NH; Mirror Lake, NH; Cushman Pond, ME; Surplus Pond, ME; Pond of Safety, NH; and Big Pea Porridge Pond, NH (Davis *et al.*, 1980; Borns *et al.*, 2004). The relatively young basal age from Ossipee Lake suggests the transition from deglaciation to the establishment of vegetation and a lake ecosystem that resembles present conditions was relatively long.

Landscape instability, indicated by elevated clastic input, persisted until 6.175 m ($\sim 9200 \pm 200$ cal yr BP; Figs. 12 & 17) representing a long period of adjustment following deglaciation. The large size of the Ossipee Lake watershed could attribute to the prolonged adjustment, as larger drainage basins in British Columbia have been shown to have extended periglacial cycles (Church & Slaymaker, 1989). The timing from the basal date (6.8 m; 11810 ± 210 cal yr BP) to the establishment of a stable landscape (6.175 m; $\sim 9200 \pm 200$ cal yr BP; Fig. 12) corresponds to reported white pine presence in the White Mountains and a low water level phase that lasted from ~ 11000 to 8000 cal yr BP (Shuman *et al.*, 2005; Oswald *et al.*, 2018). The timing of the onset of a stabilized landscape, $\sim 9200 \pm 200$ cal yr BP, aligns well with the timing of maximum vegetation coverage reported at Mirror Lake, New Hampshire from ~ 9500 to 9000 cal yr BP (Likens & Davis, 1975). This increase in vegetation was brought about by warming and increased precipitation between ~ 10000 to 8000 cal yr BP (Fig. 4), and vegetation in inland New England shifted as hemlock, birch, beech, and oak replaced white pine (Shuman *et al.*, 2005; Oswald *et al.*, 2018). Above 6.175 m, sediment properties appear relatively more stable with variations in geochemical signatures driven by event layer deposition. Despite uncertainties in the timing of the post-glacial transition, the presence of highly clastic and organically depleted sediment at the bottom of the record (Fig. 12), in addition to the transition observed in the subbottom sonar transects (Fig. 11) suggests the south basin composite record is a continuous undisturbed record from the establishment of a post-glacial environment to the summer of 2017 when the uppermost part of the core was collected.

5.5 Holocene sedimentation

From the establishment of a stable landscape ($\sim 9200 \pm 200$ cal yr BP) to present, cMAR exhibits a gentle increasing trend (Figs. 17 and 18), contrary to an expected relaxation in

sediment yield with paraglacial landscape adjustment as sediment in the landscape becomes exhausted (Ballantyne, 2002). Potentially correlated to the increased erosion over the past ~9000 years is the general increase in effective precipitation (Fig. 18). The increase in cMAR over this period highlights the role of moisture balance on long-term controls on erosion, especially considering the increased erosion is observed on a continually forested landscape.

Clusters of event layers occur in the ranges ~8500 to 7800, ~6500 to 2500, and 1600 cal yr BP to present, and are most frequent between ~9000 to 2400 cal yr BP (606 to 267 cm; Figs. 12, 17, and 18). Due to the relatively low event frequency (< 1 event per century), caution is required when interpreting variations through time. The depths and ages of the observed event layers and cMAR provide evidence for a more dynamic landscape during the mid to late Holocene, while the early Holocene has been relatively stable. Increases in K within event layers suggest sediment is sourced from unweathered or poorly weathered glacial deposits (Yellen *et al.*, 2014; Cook *et al.*, 2015), however it is difficult to directly link Ossipee Lake event layers to other lacustrine records.

Increased cMAR around ~8200 cal yr BP immediately follows a period of increased hydrologic events recorded at Ritterbush Pond, Vermont (Brown *et al.*, 2000), and agrees with increased hydrologic events recorded in lakes in New York, Vermont, New Hampshire, and Maine (Noren *et al.*, 2002; Parris *et al.*, 2010), suggesting storminess may be the reason event layer frequency in Ossipee Lake is slightly elevated during this period.

The period of increased cMAR and slightly more frequent event layers around ~6300 cal yr BP within the Ossipee Lake record aligns with increased sediment deposition recorded in New England alluvial fan trenches (Jennings *et al.*, 2003) and lake cores (Brown *et al.*, 2000; Noren *et al.*, 2002; Parris *et al.*, 2010; Fig. 18). Charcoal counts in cores from Ritterbush Pond (Brown *et*

al., 2000) are low throughout the records and do not increase around or in event layers, suggesting the more active landscape and less stable mid-Holocene environment is likely not linked to wild fire activity. Conversely, a warm and stormy mid-Holocene (Spear *et al.*, 1994) brought about by the northward expansion of warm tropical air following a cool and dry period (Parris *et al.*, 2010) could have driven increased sedimentation. Increased deposition during the mid-Holocene does not agree with hillslope stability recorded in northern Vermont (Bierman *et al.*, 1997), which was found to be more active during the early and late Holocene and relatively dormant during the mid-Holocene.

Periods of soil development recorded in Vermont fans around 5500 and 4300 cal yr BP (Jennings *et al.*, 2003) coincide with periods of low Ossipee Lake cMAR (Fig. 17 and 18). Event layers are also absent during these two periods of soil development except for Event ID 12 (Table 4; Fig. 18) at ~5600 cal yr BP, however this layer has a relatively smaller signal compared to other Ossipee event layers (Fig. 12).

Elevated cMAR and increased frequency of event layers is also observed in the Ossipee Lake record ~3000 cal yr BP, and align with increased deposition in other New England lakes (Brown *et al.*, 2000; Noren *et al.*, 2002; Parris *et al.*, 2010; Fig. 18). Jennings *et al.* (2003) conversely report a period of soil development within fans in Vermont during this period (3200 cal yr BP), interpreted as stable environmental conditions. Elevated cMAR and increased event layer frequency ~1100 cal yr BP aligns only with increased hydrologic events recorded in other New Hampshire and Maine lakes (Parris *et al.*, 2010), suggesting increased hydrologic activity during this period could be restricted to northeastern New England.

The agreement between increased sedimentation recorded in Ossipee Lake and other records around ~8200, 6000, and 3000 cal yr BP (Fig. 18) suggests environmental shifts could be

regional, potentially correlated to shifts in tropical air masses (Parris *et al.*, 2010) or low phase Arctic Oscillation associated with weakened high latitude westerlies (Noren *et al.*, 2002). However, not all periods of elevated cMAR are observed in other records, such as around ~1100 cal yr BP, and are potentially related to factors such as localized high intensity and small size storm cells or heterogeneous precipitation duration and intensity in large storms (Jennings *et al.*, 2003). Another possible mechanism influencing clastic sedimentation in the Ossipee Lake watershed could be valley widening driven by channel migration, eroding easily mobilized material. Additionally, upland erosion and alluvial fan formation following an extreme hydrologic event could result in the gradual reworking of sediment in stream valleys over time until that source of sediment is exhausted (Ballantyne, 2002).

The pattern of sedimentological properties within event layers are characteristic of discrete erosion events, characterized by a sharp onset in clastic deposition shown by a distinct color change from dark to light brown sediment, and sharp increase in bulk density, magnetic susceptibility, and K, followed by the gradual transition back to gyttja sedimentation (Cook *et al.*, 2015; Fig. 12). This pattern has been linked to discrete erosion events or single flood deposits where a short-lived, large-scale disturbance causes an initial shock to the landscape, mobilizing a relatively large amount of sediment almost immediately. Following this initial disturbance, the landscape may go through a prolonged recovery, where areas that experienced erosion are more susceptible to erosion with preceding disturbances, until the landscape recovers.

5.6 Anthropocene sedimentation

I initially expected that human activity during the 19th century would have made the Ossipee Lake watershed more susceptible to disturbances. These human activities are evident by abundance of farms and improved land (Merrill, 1889) and presence of numerous paper and saw

mills throughout Carroll county in 1861 (Fig. 9). Contrary to my prediction, only one event layer exists within the past 250 years in the Ossipee Lake record (Event ID 1; Table 4), with the onset of the layer at 33.5 cm (Fig. 12) interpreted as 60 ± 10 cal yr BP, or 1890 ± 10 (Table 6; Fig. 15). The interpreted age of this event layer is younger than suggested through ^{210}Pb modelling (~ 1870 ; Fig. 14 C) and previously reported (1841 ± 30 ; Perello, 2015). An increase in bulk Pb from 27 to 28 cm, interpreted year to coincide with ~ 1920 , combined with the onset of detectable ^{137}Cs at 14.5 cm, conversely suggests the estimated age of Event ID 1 should be ~ 1900 . Furthermore, for the age-depth models to fit the estimated age obtained through ^{210}Pb modelling and the previous study with the well constrained ^{137}Cs age-control point at 14.5 cm (Table 5), the LAR within the Event ID 1 would have to decrease, counterintuitive to the expected increase within event layers assuming they originate from increased accumulation of clastic sediment. Therefore, I interpret the onset of Event ID 1 to be younger than suggested through ^{210}Pb modelling.

The timing of the Event ID 1 does not align with recorded flooding events in the region (Thompson *et al.*, 1964), and predates the 20th century. Event ID 1 is therefore not related to late 20th century increased precipitation trends (Collins, 2009; Armstrong *et al.*, 2012; 2014) or isolated extreme flood events as observed elsewhere (Cook *et al.*, 2015). No event layers exist within the 20th century record, despite many large-magnitude floods (Fig. 3). Peak annual streamflow recorded at the Bearcamp River gage station (Fig. 3 C) shows less variation compared to the Saco River in Conway, NH (Fig. 3 D). Known high flow events (*e.g.* Tropical Storm Irene in 2011) produced discharge values in the Saco River that greatly exceed other peak annual values, whereas the discharge recorded in the Bearcamp River did not increase greatly during this event, nor does it seem to greatly influence discharge recorded in the Ossipee River

just downstream of the Ossipee Lake dam (Fig. 3 A and B). The Ossipee Lake watershed therefore appears to be less sensitive to isolated high flow events.

Peak EuroAmerican settlement within Carroll County occurred in 1860 (Merrill, 1889), and predates Event ID 1. Farmland area in New Hampshire remained elevated until 1910 (Fig. 10). The frequency of hurricanes and tropical storms at 1890 ± 10 increased from one storm per year to three (Fig. 6 in Perello, 2015). It is possible that relatively high farmland area in the watershed, combined with slight relative increase in storm frequency, led to the deposition of Event ID 1.

Grain size through the same event layer was measured by Perello (2015) in two cores from Ossipee Lake, and show no grading in mean or modal particle size. The lack of grain size gradation within the event layer suggests turbidity currents or single floods are not drivers of the recorded disturbance. In contrast, it would be possible to emplace graded event layers with a gradual decrease in clastic material and constant grain size through continuous landscape disturbances that shed sediment in decreasing amount over time as the landscape recovers from the initial disturbance. Studies focused on land use impacts on sediment yields often find more gradual increase in cMAR as land use intensifies (Davis, 1976; Dearing *et al.*, 1987; Cook *et al.*, 2015). The timing and sedimentological properties of Event ID 1 make it difficult to attribute prolonged deforestation or an isolated extreme hydrologic event to this disturbance. It is possible that wide spread farmland created a landscape more sensitive to continuous disturbances.

A potential reason for the lack of clear EuroAmerican land-use or 20th century flood signals could be the relatively large size of the Ossipee Lake watershed. Mobilized sediment from landscape disturbances could be trapped in features upstream of Ossipee Lake, such as alluvial fans (Bierman *et al.*, 1997), wetlands (Thorson *et al.*, 1998), and floodplains (James,

2019; Johnson *et al.*, 2019). Likely sediment traps could exist in the lower reaches of the Bearcamp and Lovell rivers that have low τ_b (Fig. 7) or in the middle and lower reaches on the Pine River which are predominantly wetland (Fig. 6). It is also possible that sediment mobilized from hillslopes remains on the hillslopes slightly downhill of the source location and are not delivered to the rivers or Ossipee Lake. A general deficiency of fine sediment, and relative predominance of sand in the surficial deposits of the watershed (Fig. 2), could also contribute to the absence of fine-grained event layers recorded in the distal coring locations.

Evidence suggests sedimentation over the Anthropocene is not anomalous compared to the Holocene at Ossipee Lake. There is only one event layer within the Ossipee Lake record in the past 250 years, and the second event layer does not occur until 100.5 cm (~675 cal yr BP or 1275). Furthermore, event layers throughout the entire southern composite record are described by the sharp onset of clastic sedimentation and gradual recovery, and this event layer characteristic is not unique to the uppermost and most recent core section (Fig. 12).

Clastic mass accumulation rates (cMARs) over the past 150 years exceed the average value over the past 10,000 years (Fig. 17). However, differences in age-control point resolution within the historic and prehistoric records are likely driving elevated recent cMAR. Within the historic record, decadal scale age-control resolution is measured through ^{137}Cs and ^{210}Pb techniques. The prehistoric record is constrained by millennial scale age-control availability obtained through more expensive ^{14}C techniques. Additionally, converting ^{14}C ages to calendar ages increases age error and further complicates the age-depth models. The elevated cMAR within the historic record may be more representative of actual conditions, and increased age-control resolution over the prehistoric record could result in elevated cMAR around event layers. It is difficult to compare cMAR between the historic and prehistoric records because LARs

calculated over shorter periods allow for greater rates. The discrepancy in comparing sedimentation rates in portions of the record with different age-control point resolution introduces a level of uncertainty in interpreting increased sedimentation within the past 150 years. Additionally, during some periods within the prehistoric record cMARs meet or exceed those of the historic record depending on the age-depth modelling technique applied (Fig. 17). To summarize, I suspect that differences in age-control point resolution are driving elevated recent cMAR, particularly because sedimentation properties in the top 150 years are similar to the rest of the Holocene (Fig. 12).

5.7 Future work

Further analysis of the Ossipee Lake cores could provide additional insight to factors influencing sedimentation. Additional chronologic control, LOI, and dry bulk density measurements on the north composite core would allow for more direct correlation with the southern composite core, and provide better constraints on accumulation rates throughout the lake. The extent of sedimentation across the Ossipee Lake basin could also be explored through analyses of grain size and LOI on surface grab samples that were collected along south-to-north and west-to-east transects of Ossipee Lake during the summer of 2018. Distributions of grain size throughout the lake would distinguish shelf/slope deposits from deep basin deposits. To further assess the implications of different age-depth modelling techniques on estimated sedimentation rates, additional exploration of the hybrid age-depth model could include exploring the relationship between LOI and accumulation rate and the influence of an exponential versus linear relationship on cMAR values. The southern composite record shows a slight increasing trend in cMAR through the Holocene (Fig. 18 A), which may be attributed to delta progradation which would also result in a general coarsening of sediment. Measurement on

grain size throughout the record would help to evaluate the influence on delta activity on sedimentation within the core. Grain size within event layers could be compared to typical sedimentation grain size to guide interpretation of event layers. Furthermore, measurements of grain size within Event ID 1 from numerous cores throughout Ossipee Lake could help identify the location of the disturbance.

Future work within the Ossipee Lake watershed could focus around a more in depth geomorphic analysis to provide further insight to how sediment is transported. Using τ_b as a proxy for sediment transport has been proven effective when considering bed load in gravel-bedded rivers (Wilkins & Snyder, 2011; Snyder *et al.*, 2013). This study is focused primarily on the delivery of fine-grained suspended sediment to the deep lake basin. It is likely that this material remains in suspension and transport even in areas of low τ_b . Further analysis of sediment transport within the Ossipee Lake watershed should focus on using τ_b values in addition to grain size from the deltas and event layers to calculate variations in Rouse number throughout the length of channels. Such calculations would provide a more quantitative approach to understand how the rivers can transport suspended sediment to Ossipee Lake, whereas, τ_b in this study should be viewed as providing relative changes in sediment transport capabilities between the Pine, Lovell, and Bearcamp rivers.

To understand the fate of mobilized sediment within the watershed, methods to balance the sediment budget between erosion in the watershed and deposition in the lake were explored. In an effort to estimate the volume of sediment carved by post-glacial channels, the Local Relief Model (LRM) Toolbox 10.2 for ArcGIS (Novák, 2014) was used to construct a local relief DEM within the proglacial outwash plains near Ossipee Lake (Fig. 2). Local relief compares the elevation of a specific cell to that of its surrounding cells, where negative local relief values

represent areas that are lower in elevation than its surrounding areas. The volume of sediment removed by incision of post-glacial channels was estimated by extracting all cells with negative local relief, and summing the value of each cell's area multiplied by the local relief elevation value. An estimated 0.07 km³ of sediment removed by post-glacial channels was achieved through this methodology. If all the removed sediment (0.07 km³) were delivered to Ossipee Lake, dividing this volume by lake area (13 km²) suggests the thickness of all clastic sedimentation within Ossipee Lake would be 538 cm. This estimate is much greater than the total thickness of event layers observed within the Ossipee Lake record, 143.5 cm (Table 4). The overestimation suggests that most of the mobilized sediment following channel incision is transported as bedload and could be stored in features upstream of Ossipee Lake or within the deltas. The spatial extent over which the LRM was performed could also contribute to the overestimation of sediment volume removed through channel incision, and future analysis should carefully define model boundaries to include areas carved by post-glacial rivers and exclude mountainous regions. To quantify the volume of post-glacial deposition within Ossipee Lake, analysis of the subbottom sonar transects, using software such as SonarWiz, could be performed in conjunction with the depth at which the transition to a modern lake environment is observed within the cores.

6.0 Conclusion

The historic portion of the Ossipee sediment cores was compared to the prehistoric portion to address research question 1: *Is sediment accumulation in Ossipee Lake over the past 250 years anomalous compared with the rest of the record?* Data generated for this thesis suggests sedimentation over the past 250 years is not anomalous compared to the rest of the Holocene. The average cMAR over the past 250 years is 0.045 g/cm²/yr, which is surpassed on

numerous occasions throughout the record depending on the age-depth model applied (Fig. 17). Furthermore, periods throughout the record meet or exceed one event over 250 years, 0.004 events/year or 0.4 events/century (Fig. 18 B), and similar sedimentological properties of event layers are observed throughout the record (Fig. 12). Linear accumulation rates and cMARs over the past 150 years are elevated compared to the prehistoric record (Figs. 16 and 17), however, differences in age-control resolution makes it difficult to compare rates from the decadal scale resolution within the historic record to the millennial scale resolution within the prehistoric record. Since short-term variations in accumulation rate are likely underrepresented during the Holocene, it is difficult to argue that sedimentation over the past 150 years is remarkable.

It is difficult to confidently answer research question 2: *Is the primary driver of watershed erosion over the past 250 years deforestation and anthropogenic changes to the landscape, or intense flooding modulated by antecedent moisture and large scale storms associated with increased precipitation trends?* Despite a documented history of EuroAmerican settlement within the Ossipee Lake watershed (Figs. 9 and 18; Merrill, 1889) and evidence for sediment delivery to Ossipee Lake (Figs. 5 and 7), an unambiguous land-use signal is not observed within Ossipee Lake sediment cores (Figs. 12 and 17). The sharp onset of clastic deposition associated within the uppermost event layer (Fig. 12) suggests the disturbance causing this layer was a discrete erosion event rather than prolonged deforestation (Cook *et al.*, 2015). The timing of this layer ($\sim 1890 \pm 10$) is well constrained through bulk Pb and ^{137}Cs analyses (Fig. 14), and postdates maximum EuroAmerican settlement within Carroll County (Merrill, 1889), but occurs during the period of wide spread farmland in New Hampshire (Fig. 10). The uppermost event layer predates a clear flood signal associated with increased precipitation trends since the late 20th century (Collins, 2009; Armstrong *et al.*, 2012; 2014). The absence of event

layers since the turn of the 20th century combined with the relatively muted response of the Bearcamp River during major flood events (Fig. 3) suggests the Ossipee Lake watershed may be less sensitive recent flooding. The lack of a clear land-use or 20th century flood signal makes it difficult to identify the primary driver of watershed erosion over the past 250 years.

The application of the CLAM, two Bacon models, and the hybrid model allow for the direct comparison of estimated ages and LARs between the different modelling techniques to address research question 3: *What implications do different age-depth modelling techniques have on estimated sedimentation rates and inferred watershed erosion rates?* The age-depth modelling techniques generally agree in estimated ages and LARs except within and immediately surrounding event layers (Figs. 15 and 16). Methods that do not account for changes in sedimentation within event layers underestimate variations in cMAR associated with event layers. Bacon with event layers accounts for variations in sedimentation within event layers, but the depths and magnitude of sedimentation within event layers are subjective. Using the hybrid model, variations in cMAR within event layers change as a function of dry bulk density and organic composition. Further work is required to test and refine this modelling technique, however the hybrid age-depth model can potentially provide a method to more realistically account for variations in sedimentation dependent on sediment properties, thus reducing user subjectivity. It is important to consider accumulation data (LARs and cMARs) are based on the median estimated age at any given depth and uncertainty ranges are not propagated through accumulation rate calculations.

The full and continuous sediment record obtained during this thesis allows for the exploration of research question 4: *How have inferred watershed erosion rates varied through the entire post-glacial period?* Changes in sediment properties and relatively high frequency of

event layers provide evidence that the disturbances over the prehistoric record may have been greater or more frequent than those within the historic record (Figs. 12 and 18). Periods with event layers are especially focused ~8500 to 7800, ~6500 to 2500, and 1600 cal yr BP to present (Figs. 17 and 18), suggesting the Ossipee Lake watershed during the mid-Holocene was subjected to more frequent disturbances. The timing of Ossipee Lake event layers align with some, but not all, periods of increased hydrologic events from other regional studies (Brown *et al.*, 2000; Noren *et al.*, 2002; Parris *et al.*, 2010). The discrepancy between events recorded in Ossipee Lake and other watersheds in New England (Brown *et al.*, 2000; Noren *et al.*, 2002; Parris *et al.*, 2010) highlight some of the difficulties in using lakes as archives of environmental change over regional spatial scales, since differences in drainage basin and lake characteristics and localized precipitation can influence sedimentation within lakes.

Results from this thesis suggest sediment delivery to Ossipee Lake is highly variable throughout the Holocene. Clastic accumulation of sediment was greatest between 9000 and 2400 cal yr BP (Fig. 18 A and B), suggesting the Ossipee Lake watershed landscape was most active during the mid-Holocene. The general increase in cMAR following the establishment of a stable landscape (Fig. 18 A) mirrors increasing effective precipitation (Fig. 18 D). However, sedimentation over the historic record is not anomalous to the rest of the record, suggesting anthropogenic activity is not significantly impacting sedimentation within Ossipee Lake.

References

- Appleby, P. G., Oldfield, F. (1978). The calculation of lead-210 dates assuming a constant rate of supply of unsupported ZloPh to the sediment. *Catena*, 5, 1-8.
- Armstrong, W. H., Collins, M. J., Snyder, N.P. (2014). Hydroclimatic flood trends in the northeastern United States and linkages with large-scale atmospheric circulation patterns. *Hydrological Sciences Journal*, 59(9), 1636-1655. DOI:10.1080/02626667.2013.862339
- Armstrong, W. H., Collins, M. J., Snyder, N.P. (2012). Increased frequency of low-magnitude floods in New England, *Journal of the American Water Resources Association*, 48(2), 307-320. DOI:10.1111/j.1752-1688.2011.00613.x
- Ballantyne, C.K. (2002). A general model of paraglacial landscape response. *The Holocene*, 12(3), 371-376.
- Bierman, P., Lini, A., Zehfuss, P., Church, A. (1997). Postglacial ponds and alluvial fans: Recorders of Holocene landscape history. *GSA Today*, 7(10), 1-7.
- Bierman, P. R., Howe, J., Stanley-Mann, E., Peabody, M., Hilke, J., Massey, C. A. (2005), Old images record landscape change through time. *GSA Today*, 15(4), 4-10. DOI:10.1130/10525173(2005)015<4.OIRLCT>2.0.CO;2
- Blaauw, M. (2010). Methods and code for 'classical' age-modelling of radiocarbon sequences, *Quaternary Geochronology*, 5, 512-518. DOI:10.1016/j.quageo.2010.01
- Blaauw, M., & Christen, J. A. (2011). Flexible paleoclimate age-depth models using an autoregressive gamma process. *Bayesian Analysis*, 6(3), 457-474.
- Borns, H. W. Jr., Doner, L. A., Dorion, C. C., Jacobson, G. L., Kaplan, M. R., Kreutz, K. J., Lowell, T. V., Thompson, W. B., Weddle, T. K. (2004). The Deglaciation of Maine, U.S.A. *Developments in Quaternary Sciences*, 2, 89-109.
- Brown, S. L., Bierman, P. R., Lini, A., Southon, J. (2000). 10 000 yr record of extreme hydrologic events. *Geology*, 28(4), 335-338.
- Brown, S. L., Bierman, P. R., Lini, A., Thompson Davis, P. (2002). Reconstructing lake and drainage basin history using terrestrial sediment layers: Analysis of cores from a post glacial lake in New England, USA. *Journal of Paleolimnology*, 28, 219-236.
- Church, M., Slaymaker, O. (1989). Disequilibrium of Holocene sediment yield in glaciated British Columbia. *Nature*, 337(6206). 452-454.
- Collins, M. J. (2009). Evidence for changing flood risk in New England since the late 20th century. *Journal of the American Water Resources Association*, 45(2), 279.

- Cook, T. L., Yellen, B. C., Woodruff, J. D., Miller, D. (2015). Contrasting human versus climatic impacts on erosion. *Geophysical Research Letters*, 42(16), 1-8.
DOI:10.1002/2015GL064436
- Davis, M. B. (1976). Erosion rates and land-use history in southern Michigan. *Environmental Conservation*, 3(2), 139-148.
- Davis, M. B., Spear, R. W., Shane, L. C. K. (1980). Holocene climate of New England. *Quaternary Research*, 14, 240-250.
- Davis, R. B., Anderson, D. S., Dixit, S. S., Appleby, P. G., Schauffler, M. (1994). Responses of two New Hampshire (USA) lakes to human impacts in recent centuries. *Journal of Paleolimnology*, 35, 669-697.
- Dean Jr, W. E. (1974). Determination of carbonate and organic matter in calcareous sediments and sedimentary rocks by loss on ignition: comparison with other methods. *Journal of Sedimentary Research*, 44(1).
- Dearing, J. A., Hakansson, H., Liedberg-Jonsson, B., Persson, A., Skanjo, S., Widholm, D., El Daoushy, F. (1987). Lake sediment used to quantify the erosional response to land use change in Southern Sweden. *Oikos*, 50(1), 60-78.
- Dearing, J. A. (1999). Using the Bartington MS2 system In *Environmental magnetic susceptibility* (pp.2-54).
- Donnelly, J. P., Hawkes, A. D., Lane, P., MacDonald, D., Shuman, B. N., Toomey, M. R., van Hengstum, P. J., Woodruff, J. D. (2015), Climate forcing of unprecedented intense hurricane activity in the last 2000 years. *Earth's Future*, 3, 49-65.
DOI:10.1002/2014EF000274
- Dunne, T., Moore, T. R., Taylor, C. H. (1975). Recognition and prediction of runoff producing zones in humid regions, *Hydrological Sciences Bulletin*, 20(3), 305-327.
- Dunne T, Leopold LB. 1978. *Water in Environmental Planning*. W.H. Freeman and Company: New York; 818.
- Favaro, E. A., Lamoureux, S. F. (2014). Antecedent controls on rainfall runoff response and sediment transport in a high Arctic catchment. *Swedish Society for Anthropology and Geography*, 96(4), 433-446. DOI:10.1111/geoa.12063
- Foster, D. R. (1992). Land-Use History (1730-1990) and Vegetation Dynamics in Central New England, USA. *Journal of Ecology*, 80(4), 753-771.
- Goldthwait, J. W., Goldthwait, R. P., Goldthwait, L., Lougee, R. J., Meyers, T. R., Page, L. R., White, G. W., and others. (1950). *Surficial Geology of New Hampshire [map]*. color, scale 1: 250,000

- Groisman, P. Y., Knight, R. W., Karl, T. R. (2001). Heavy precipitation and high streamflow in the contiguous United States: Trends in the 20th century. *Bulletin of the American Meteorological Society*, 1-44.
- Groisman, P. Y., Knight, R. W., Karl, T. R., Easterling, D. R. (2004). Contemporary changes in the hydrologic cycle over the contiguous United States: Trends derived from in situ observations. *Journal of Hydrometeorology*, 5, 64-85.
- Hooke, R. L. (1994). On the efficacy of humans as geomorphic agents. *GSA Today*, 4(9), 217, 224-225.
- Hooke, R. L. (2012). Land transformation by humans: A review. *GSA Today*. 22(12), 4-10. DOI:10.1130/GSAT151A.1.
- Intergovernmental Panel on Climate Change (IPCC), 2014: Climate Change 2014: Synthesis Report. Contribution of Working Groups I, II and III to the Fifth Assessment Report of the Intergovernmental Panel on Climate Change [Core Writing Team, R.K. Pachauri and L.A. Meyer (eds.)]. IPCC, Geneva, Switzerland.
- James, L. A. (2019). Legacy sediment: Definitions and processes of episodically produced anthropogenic sediment. *Anthropocene*, 2(2013), 16-26.
- Jennings, K. L., Bierman, P. R., Southon, J. (2002). Timing and style of deposition on humid temperate fans, Vermont, United States. *GSA Bulletin*, 115(2), 182 – 199.
- Johnson, K. M., Ouimet, W. B. (2014). Rediscovering the lost archaeological landscape of southern New England using light detection and ranging (LiDAR). *Journal of Archaeological Science*, 43, 9-20.
- Johnson, K. M., Snyder, N. P., Castle, S., Hopkins, A. J., Waltner, M., Merritts, D. J., Walter, R. C. (2018). Legacy sediment in New England river valleys: Anthropogenic processes in a postglacial landscape. *Geomorphology*, 327(2019), 417-437.
- Luce, D. L. (2012). *Sediment metal concentrations as a function of land use in the Charles River, Eastern Massachusetts*. (Doctoral Dissertation). University of Massachusetts Boston, Boston, MA.
- Likens, G. E., Davis, M. B. (1975). Post-glacial history of Mirror Lake and its watershed in New Hampshire, U.S.A.: an initial report, *Verh. Internat. Verein. Limnol.* 19, 982-993.
- Marsicek, J.P., Shuman, B.P., Brewer, S., Foster, D.R., Oswald, W.W. (2013). Moisture and temperature changes associated with the mid-Holocene Tsuga decline in the northeastern United States. *Quaternary Science Reviews*, 80, 129-142. DOI:10.1016/j.quascirev.2013.09.001
- Marlon, J. R., Pederson, N., Nolan, C., Goring, S., Shuman, B., Robertson, A., . . . Yu, Z. (2017). Climatic history of the northeastern United States during the past 3000 years. *Climate of the Past*, 13, 1355-1379.

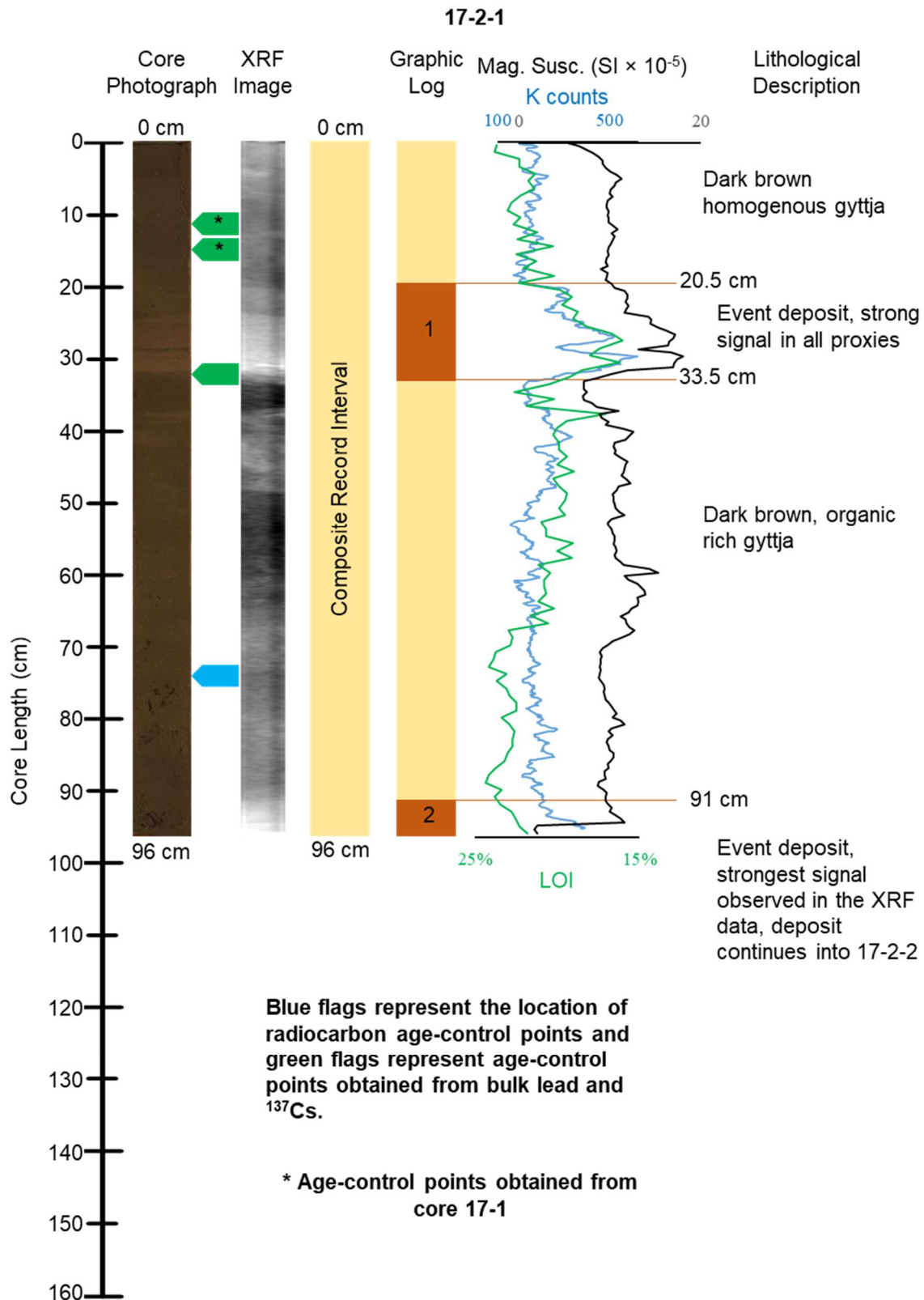
- Medalie, L., Moore, R. B. (1995). Ground-water resources in New Hampshire: Stratified drift Aquifers. Bow, N.H.: U.S. Dept. of the Interior, U.S. Geological Survey.
- Merrill, G. Drew. (1889). History of Carroll County, New Hampshire. Boston, MA: W.A. Fergusson & Co.
- Minderhoud, P. S. J., Cohen, K. M., Toonen, W. H. J., Erkens, G., Hoek, W. Z. (2016). Improving age-depth models of fluvio-lacustrine deposits using sedimentary proxies for accumulation rates. *Quaternary Geology*, 33, 35-45.
- Moore, R. B., Medalie, L. (1995). Geohydrology and water quality of stratified-drift aquifers in the Saco and Ossipee River Basins, east-central New Hampshire. Bow, N.H.: U.S. Dept. of the Interior, U.S. Geological Survey.
- Munoz, S. E., Gajewski, K., Peros, M. C. (2010). Synchronous environmental and cultural change in the prehistory of the northeastern United States. *PNAS*, 107(51), 22008-22013.
- New Hampshire Department of Environmental Services. (2017). Volunteer Lake Assessment Program Individual Lake Reports. Ossipee Lake. Published by the New Hampshire Department of Environmental Services: Concord NH.
- University of New Hampshire, Complex Systems Research Center. (2002). New Hampshire Land Cover Assessment. New Hampshire GRANIT, Durham, NH.
- Newby, P. E., Shuman, B. N., Donnelly, J. P., MacDonald, D. (2011). Repeated century-scale droughts over the past 13,000 yr near the Hudson River watershed, USA. *Quaternary Research*, 75(3), 523-530. DOI: 10.1016/j.yqres.2011.01.006
- Newby, P. E., Shuman, B. N., Donnelly, J. P., Karnauskas, K. B., Marsicek, J. (2014). Centennial-to-millennial hydrologic trends and variability along the North Atlantic Coast, USA, during the Holocene, *Geophysical Research Letters*, 41, pp.4300-4307.
- Newby, P.E., Shuman, B.N., Donnelly, J.P., MacDonald, D. (2011). Repeated century-scale droughts over the past 13,000 yr near the Hudson River watershed, USA. *Quaternary Research*, 75(3), 523-530. DOI:10.1016/j.yqres.2011.01.006
- Newell, A. E. (1960). *Biological survey of the lakes and ponds in Coos, Grafton and Carroll counties* (Survey Report No. 8a). New Hampshire Fish and Game Department.
- Newton, R. M. (1974a). Surficial Geology of the Ossipee Lake Quadrangle, New Hampshire. Concord, State of New Hampshire, Dept. of Resources and Economic Development, Concord, NH.
- Newton, R. M. (1974b) Surficial Geologic Map of the Ossipee Lake quadrangle, New Hampshire [map]. color, scale 1:62,500.

- NH Department of Environmental Services. (2019, January 15). *Stone wall mapping project uses new technology to honor the past*. Retrieved from <https://www.des.nh.gov/media/pr/2019/20190115-stone-wall-mapping.htm>
- Noren, A. J., Bierman, P. R., Steig, E. J., Lini, A., Southon, J. (2002). Millennial-scale storminess variability in the northeastern United States during the Holocene epoch. *Letters to Nature*, 419, pp.812-824.
- Normandeau, A., Lamoureux, S. F., Lajeunesse, P., Francus, P. (2016). Sediment dynamics in paired High Arctic lakes revealed from high-resolution swath bathymetry and acoustic stratigraphy surveys. *Journal of Geophysical Research*, 121(9), 1676-1696.
- Novák, David. (2014). Local Relief Model (LRM) Toolbox for ArcGIS (UPDATE 2016-05 - new download link). 10.13140/RG.2.1.2010.1201/1.
- Nowaczyk, N. R. (2001) In Last, W. M., Smol, J. P. *Tracing environmental change using lake sediments volume 1: basin analysis, coring, and chronological techniques* (pp.155-170) Dordrecht, The Netherlands: Kuwer Academic Publishers.
- Oswald, W. W., Foster, D. R., Shuman, B. N., Doughty, E. D., Faison, E. K., Hall, B. R., ... Truebe, S. A. (2018). Subregional variability in the response of New England vegetation to postglacial climate change, *Journal of Biogeography*, 45, 2375-2388. DOI:10.1111/jbi.13407
- Parris, A. S., Bierman, P. R., Noren, A. J., Prins, M. A., Lini, A. (2010). Holocene paleostorms identified by particle size signatures in lake sediment from northeastern United States. *Journal of Paleolimnology*, 43, 29-40. DOI 10.1007/s10933-009-9311-1
- Perello, M. (2015). *Linking the effects of land use vs. climate change on water quality in Ossipee and Squam Lakes, NH* (Master's thesis). Plymouth State University, Plymouth, NH.
- Perkins, R. W., & Thomas, C. W. Hanson, W. C. (1980). *Worldwide fallout*. Oak Ridge, TN: Technical Information Center.
- Ramsey, C. B., (2008). Deposition models for chronological records. *Quaternary Science Reviews* 27, 42-60.
- Reimer, P. J., Bard, E., Bayliss, A., Beck, J. W., Blackwell, P.G., Ramsey, C. B., ... van der Plicht, J. (2013) IntCal13 and Marine13 radiocarbon age calibration curves 0-50,000 yr cal BP. *Radiocarbon*, 55(4), 1869-1887.
- Renshaw, C. E., Magilligan, F. J., Doyle, H. G., Dethier, E. N., Kantack, K. M. (2019). Rapid response time of New England (USA) rivers to shifting boundary conditions: Processes, time frames, and pathways to post-flood channel equilibrium. *Geology*, 47(20), 997-1000.
- Ridge, J. C., Balco, G., Bayless, R. L., Beck, C. C., Carter, L. B., Dean, J., Voytek, E. B., Wei, J.H. (2012). The new North American Varve Chronology: A precise record of

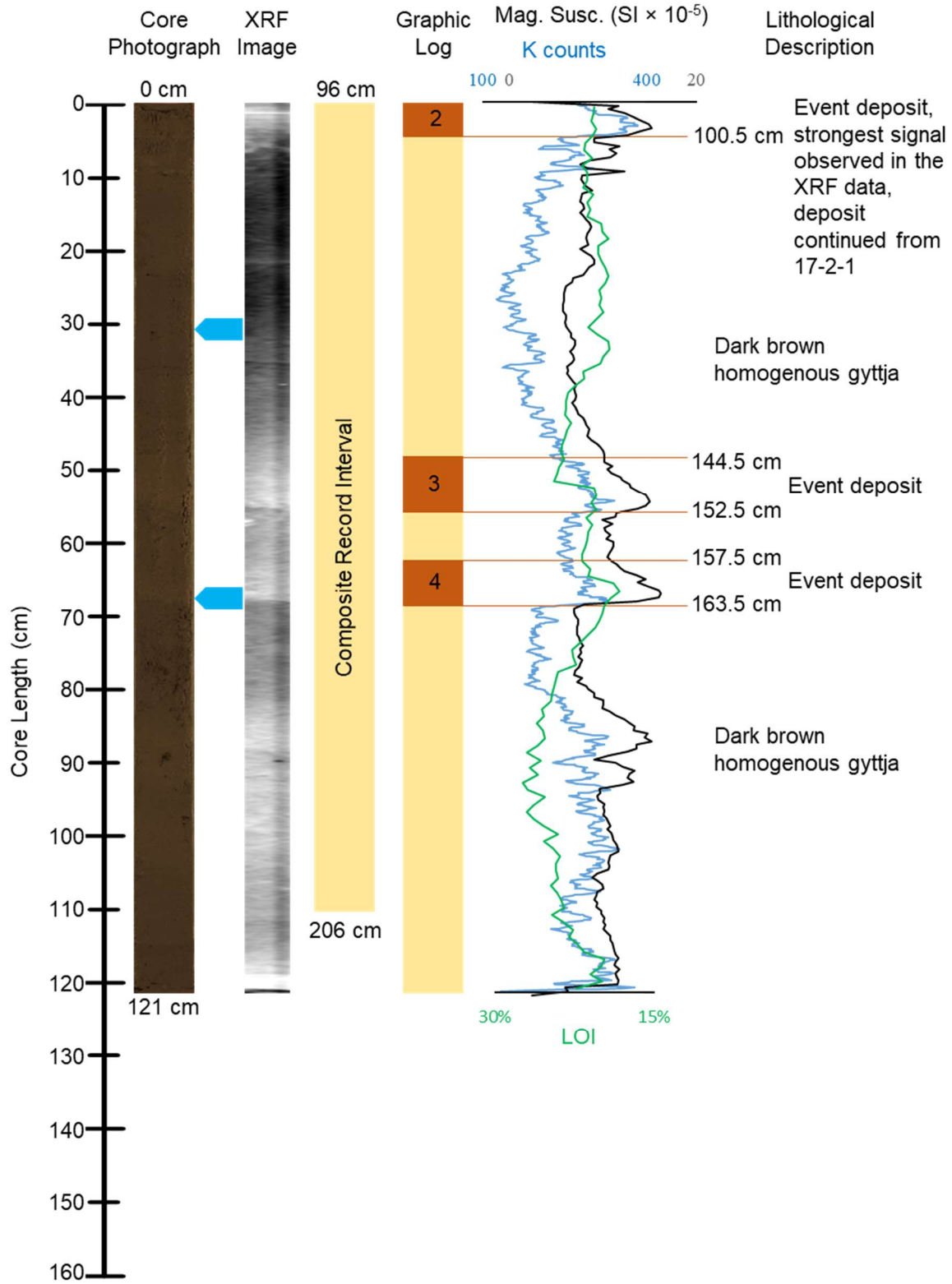
- southeastern Laurentide Ice Sheet deglaciation and climate, 18.2-12.5 kyr BP, and correlations with Greenland ice core records. *American Journal of Science*, 312, 685-722. DOI:10.2475/07.2012.01
- Ritchie, J. C., McHenry, J. R. (1990). Application of radioactive fallout Cesium-137 for measuring soil erosion and sediment accumulation rates, *Journal of Environmental Quality*, 19, 215-233.
- Sachs, J.P. (2008). Cooling of Northwest Atlantic slope waters during the Holocene. *Geophysical Research Letters*, 34, L03609. DOI:10.1029/2006GL028495
- Schiff, R., MacBroom, J. G., Armstrong Bonin, J. (2007) Guidelines for Naturalized River Channel Design and Bank Stabilization. NHDES-R-WD-06-37. Prepared by Milone & MacBroom, Inc. for the New Hampshire Department of Environmental Services and the New Hampshire Department of Transportation, Concord, N.H.
- Shuman, B., Newby, P., Donnelly, J. P., Tarbox, A., Webb, T. (2005). A record of Late Quaternary moisture-balance change and vegetation response from the White Mountains, New Hampshire. *Annals of the Association of American Geographers*, 95(2), 237-248.
- Snyder, N. P., Whipple, K. X., Tucker, .G. E, Merritts, D. J. (2003). Channel response to tectonic forcing: field analysis of stream morphology in the Mendocino triple junction region, northern California. *Geomorphology*, 53, 97–127. DOI: 10.1016/S0169-555X(02)00349-5
- Snyder, N. P. (2009). Studying stream morphology with airborne laser elevation data, *Eos, Transactions, American, Geophysical Union*, 90(6), 45-52. DOI: 10.1029/2009EO060001.
- Snyder, N. P., Neshheim, A. O., Wilkins, B. C., Edmonds, D. A. (2013). Predicting grain size in gravel-bedded rivers using digital elevation models: Application to three Maine watersheds, *GSA Bulletin*, 125(1), 148-163. DOI: 10.1130/B30694.1
- Spear, R. B., Davis, M. B., Shane, L. C. (1994). Late quaternary history of low- and mid-elevation vegetation in the White Mountains of New Hampshire. *Ecol Monogr*, 64, 85-109. DOI:10.2307/2937056
- Sperduto, D. D., Nichols, W. F. (2004). Natural Communities of New Hampshire. NH Natural Heritage Bureau, Concord, NH. Pub. UNH Cooperative Extension, Durham, NH.
- Thompson, M. T., Gannon, W. B., Thomas, M. P., Hayes, T. G. (1964). Historical floods in New England, Geological Survey Water-Supple Paper 177-M, United States Government Printing Office, Washington, D. C.
- Thompson, W. B., Fowler, B. K. & Dorion, C. C. (1999). Deglaciation of the north-western White Mountains, New Hampshire. In: Thompson, W.B., Fowler, B.K. & Davis, T. (eds), Late Quaternary history of the White Mountains, New Hampshire and adjacent south-eastern Québec. *Géographie physique et Quaternaire*, 53, 59-77.

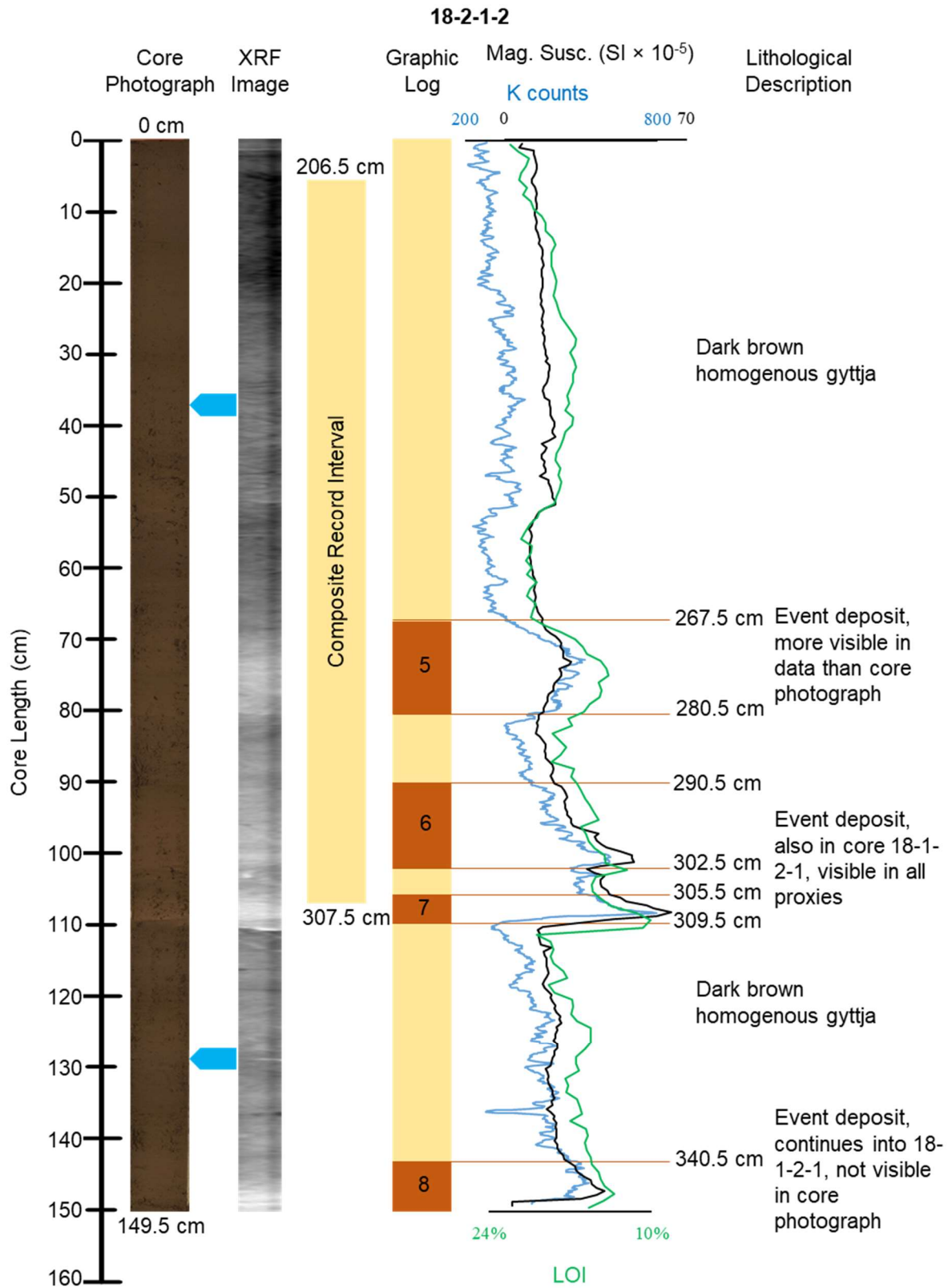
- Thorson, R. M. Harris, A. G., Harris, S. L., Gradie, R., Lefor, M. W. (1998). Colonial impacts to wetlands in Lebanon, Connecticut. *GSA Reviews in Engineering Geology*, 12, 23-42.
- Trachsel, M., Telford, R. J. (2017). All age-depth models are wrong, but are getting better. *The Holocene*, 27(6), 860-869. DOI: 10.1177/0959683616675939
- Viau, A. E., Gajewski, K., Sawada, M. C., Fines, P. (2006). Millennial-scale temperature variations in North America during the Holocene. *Journal of Geophysical Research*, 11, 1-12. DOI:10.1029/2005JD006031
- Walling, D. E. (2004). Using environmental radionuclides to trace sediment mobilisation and delivery in river basins as an aid to catchment management *in* Proceedings of the Ninth International Symposium on River Sedimentation, 121-135.
- Ward, P. J., van Balen, R. T., Verstraeten, G., Renssen, H., Vandenberghe, J. (2009). The impact of land use and climate change on late Holocene and future suspended sediment of the Meuse Catchment, *Geomorphology*, 103, 389-400. DOI:10.1016/j.geomorph.2008.07.006
- Woodford, E. M. & Smith & Peavey. (1861) *Topographical map of Carroll County, New Hampshire*. New York: Smith & Peavey. [Map] Retrieved from the Library of Congress, <https://www.loc.gov/item/2012587750/>.
- Wilkins, B. C., Snyder, N. P. (2011). Geomorphic comparison of two Atlantic coastal rivers: toward an understanding of physical controls on Atlantic salmon habitat. *River and Research Applications*, 27, 135-156. DOI: 10.1002/rra.1343.
- Wilson, J. R. (1937) *The geology of the Ossipee Lake quadrangle, New Hampshire*. Concord, New Hampshire: New Hampshire Department of Resources and Economic Development.
- Yellen, B., Woodruff, J. D., Kratz, L. N., Mabee, S. B., Morrison, J., Martini, A. M. (2014). Source, conveyance, and fate of suspended sediments following Hurricane Irene, New England, USA. *Geomorphology*, 226, 124-134.
- Yellen, B., Woodruff, J. D., Cook, T. L., Newton, R. M. (2016) Historically unprecedented erosion from Tropical Storm Irene due to high antecedent precipitation. *Earth Surface Processes and Landforms*, 41, 677-684. DOI: 10.1002/esp.3896
- Zhang, X. C., Zhang, G. H., Garbrecht, J. D., Streiner, J. L. (2015). Dating sediment in a fast sedimentation reservoir using cesium-137 and lead-210. *Soil and Water Management & Conservation*, 79(3), 948-956. DOI: 10.2136/sssaj2015.01.0021

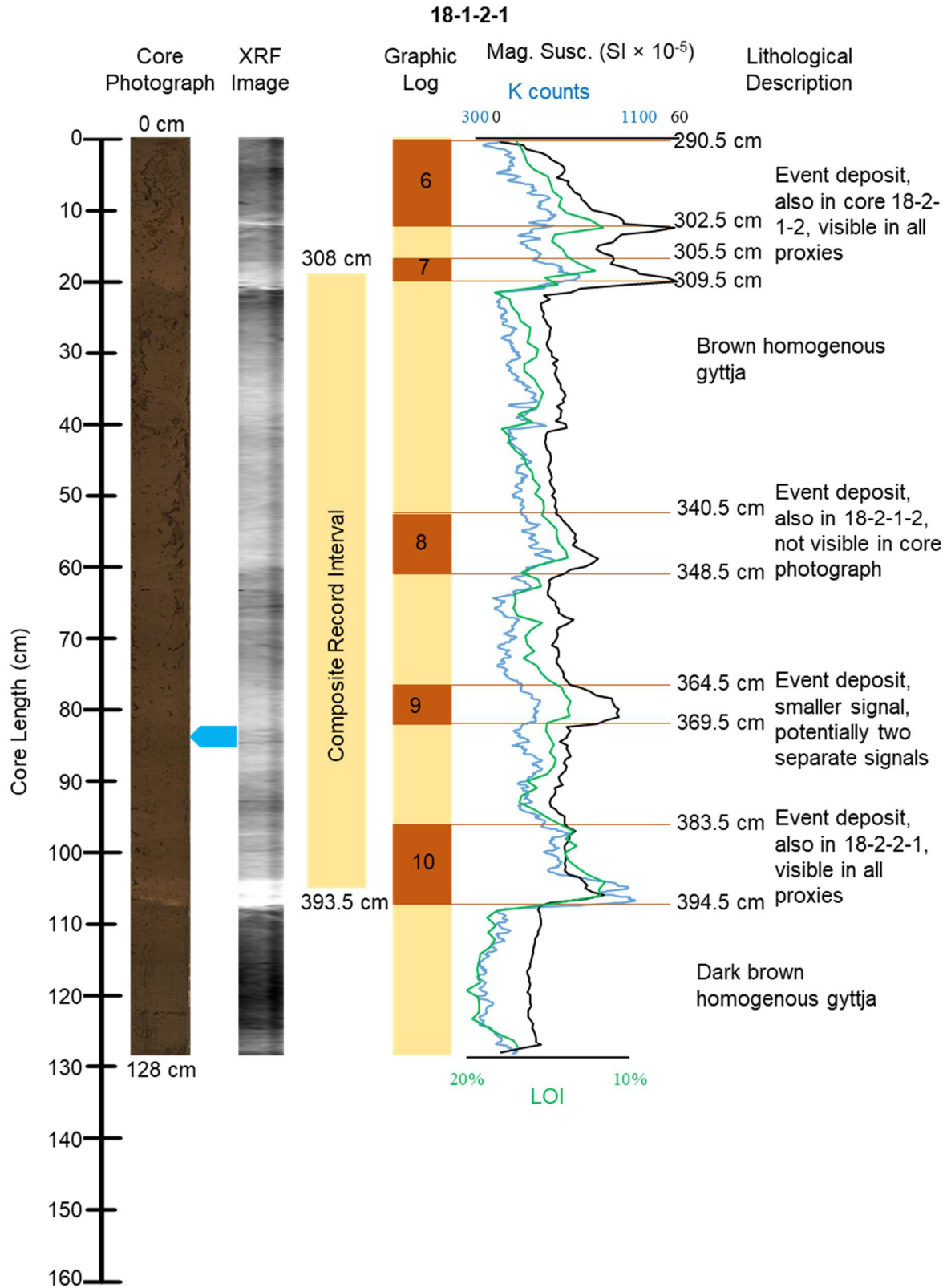
Appendix. Section cores that comprise the Ossiipee Lake southern composite record

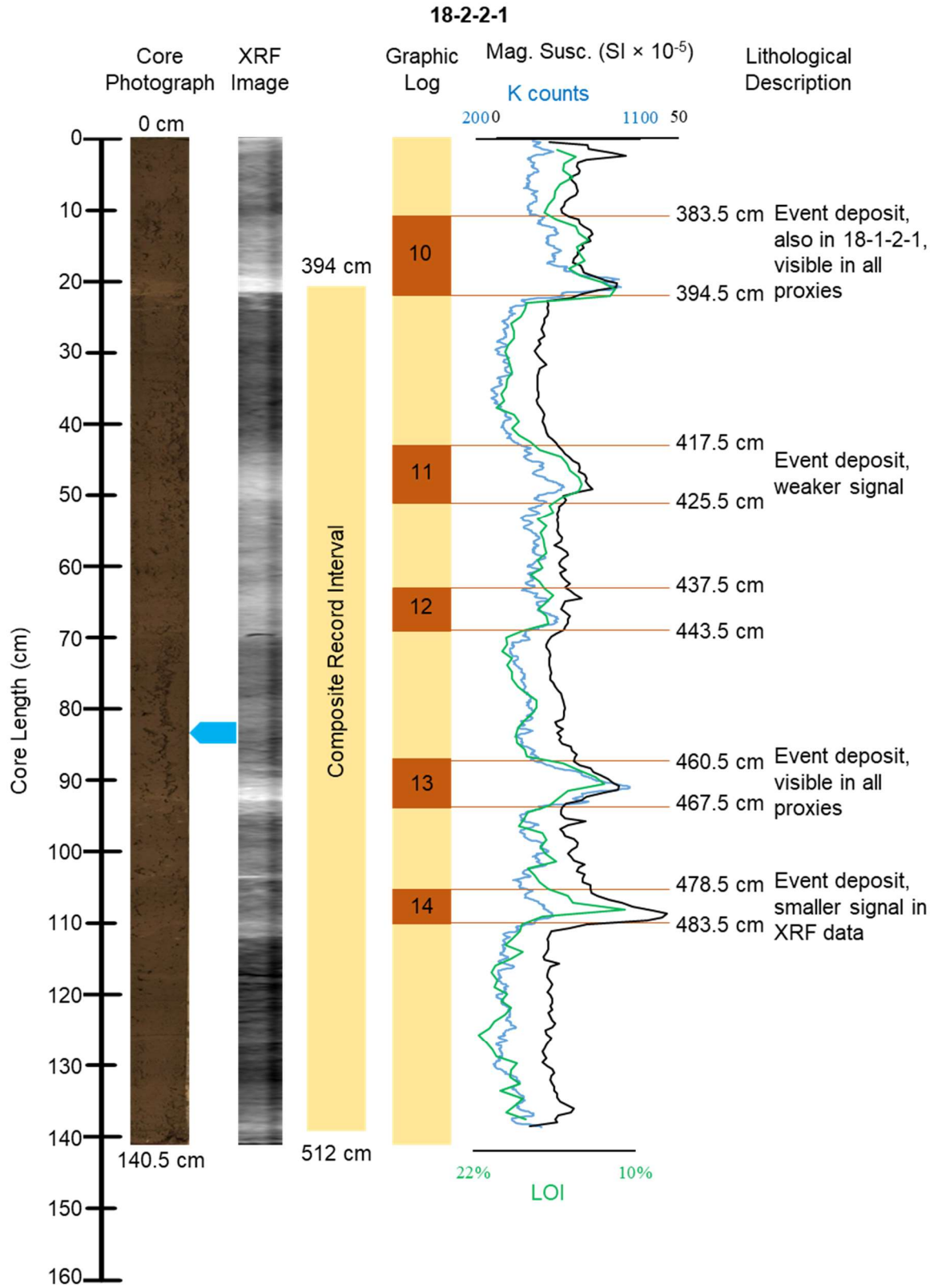


17-2-2

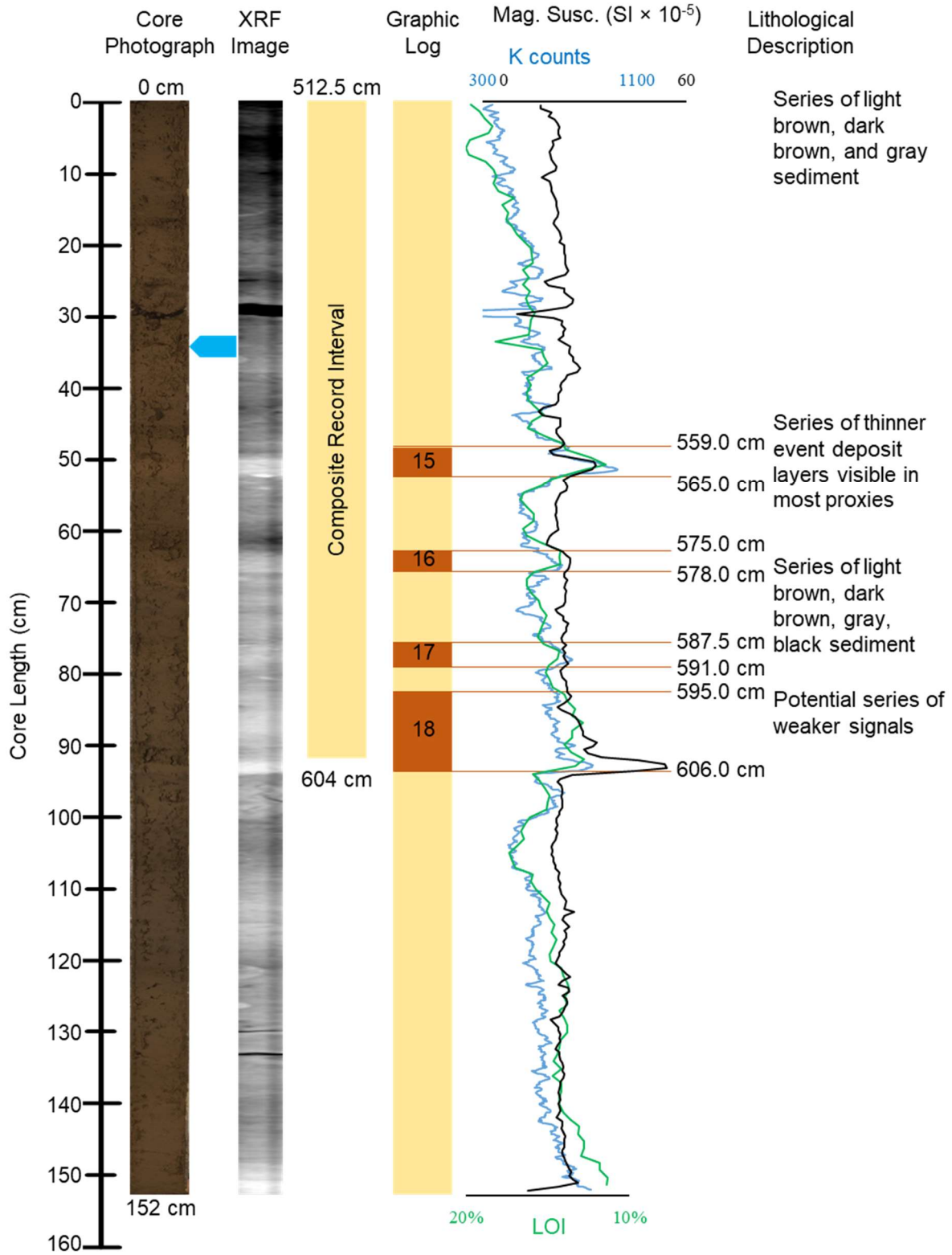








18-2-2-2



18-1-3-1

